MUHAMMAD UZAIR
IMPLEMENTATION OF SPACE–VECTOR-MODULATION IN A THREE-PHASE VSI-TYPE GRID-CONNECTED INVERTER

Master of Science thesis

ABSTRACT

TAMPERE UNIVERSITY OF TECHNOLOGY
Master's Degree Programme in Electrical Engineering
MUHAMMAD UZAIR: Implementation of space-vector-modulation in three-phase VSI-type grid-connected inverter.
Master of Science Thesis, 49 pages, 13 Appendix pages
September 2015
Major: Smart Grids
Examiner: Professor Teuvo Suntio

Keywords: SVPWM, THD, VSI, NPC, stationary vectors.

The motivation behind this thesis is to generate AC signal of varying amplitude and frequency from a constant DC source. The device which is used to obtain this kind of action is known as inverter. At present, the inverter is classified into three ways i.e. square wave inverter, modified sine wave inverter or quasi sine wave inverter and pure sine wave inverter. The first two classification of inverter have seldom used and have very limited applications. Nowadays, the pure sine wave inverter is more demanding because of the requirement of high efficiency and reliability. On the contrary, it is more complex to implement. The main focus of this thesis is the implementation of space vector-pulse-width-modulation (SVPWM) which is one of the algorithm of different pulse-width-modulation techniques. It is applicable for three phase voltage-source-inverter for controlling induction and synchronous machine. In this technique, the reference vector of varying amplitude and direction continually revolve around the hexagon with a fixed sampling frequency generating a gate pulses for the 12 power switches used in neutral-point-converter. The space-vector-pulse-width-modulation is advantageous over carrier based pulse-width-modulation. The properties which are used to analyze the performance of different pulse width modulation methods are total harmonic distortion (THD) and the amplitude of fundamental component. Better utilization of DC bus voltage makes the space-vector-pulse-width-modulation better than the carrier based pulse-width-modulation.

This thesis explains the concept, theory and implementation of three level space-vector pulse-width modulation using MATLAB/Simulink environment. It also incorporates the waveform of 7-segment, 9 segment and 13-segment switching pattern to avoid the problem of harmonics. The concept of DC-neutral-point-potential control has also been developed. To support the theory, gating signal pattern has been drawn and some mathematical calculations have been performed. To get the clear picture of voltage measurement at each output stage, the derivation of line-to-line voltages and line-to-neutral voltages are also taken into account along with the calculation of duty cycle of switches.

PREFACE

I would like to express my sincere gratitude and thanks to my supervisor Prof. Teuvo Suntio for giving me this precious opportunity to work under his supervision. Without him I wouldn't able to achieve this goal. His guidance and kind advice filled me with enthusiasm which helped me to achieve this milestone.

I would also like to appreciate the effort made by my true friend Mr. Umair Fatimi for his kind assistance throughout my thesis.

Last but not least I am very much thankful to my parents and brothers for their moral support in every stage of my entire life.

Tampere, 20.09.2015

Muhammad Uzair

CONTENTS

APPENDIX I: *Implementation of conversion of three phase quantities to stationary reference frame.*

APPENDIX II: *Mathematical model of "Sector selection block".*

APPENDIX III: *Mathematical model of "Region selection block".*

APPENDIX IV: *Mathematical model of "Dwell time calculation block".*

APPENDIX V: *Analysis of Y-φ a) FFT window of Y- φ b) Harmonic analysis of Y-φ.*

APPENDIX VI: *Analysis of B-φ a) FFT window of B- φ b) Harmonic analysis of B-φ.*

APPENDIX VII: *Analysis of Y- φ current a) current waveform b) Harmonic analysis.*

APPENDIX VIII: *Analysis of B- φ current a) current waveform b) Harmonic analysis.*

APPENDIX IX: *Switching schemes for sector II, III, IV, V and VI.*

APPENDIX X: *a) Simulink model of 3-level inverter b) power stage of the inverter.*

LIST OF FIGURES

LIST OF TABLES

LIST OF SYMBOLS AND ABBREVIATIONS

AC   Alternating Current
DC   Direct Current
DCMC   Diode Clamped Multilevel Converter
DSP   Digital Signal Processor
FCMC   Flying Capacitor Multilevel Converter
IGBT   Insulated Gate Bipolar Transistor
mmf   Magnetomotive Force
NPC   Neutral Point Converter
PWM   Pulse Width Modulation
SVC   Static VAR Compensator
SVG   Static VAR Generator
SVPWM   Space Vector Pulse Width Modulation
THD   Total harmonic Distortion
UPS   Uninterruptable Power Supply
VSI   Voltage Source Inverter

α real axis
β imaginary axis
F   magnetomotive Force
i_R R-phase current
θ_{ae} angle between the produced magnetic field w.r.to its axis
1   fundamental component
ω angular velocity
V_{ref} reference voltage
m   modulation index
d   duty cycle

.

1. INTRODUCTION

1.1 Background

From the last two decades or so, the growth in the renewable energy sources has increased tremendously which leads to increase the demand of power electronics converter. Energy generated from renewable energy like wind, wave and photovoltaic are heavily dependent on power converters as they are not capable of producing such amount of power that the grid can stand with it. The power generated from these renewable sources cannot directly connect to the grid; it needs to meet some criteria by means of frequency, phase and amplitude. To meet the demand of grid need to incorporate some sort of device which is capable of providing such amount of power the grid will able to handle. Here, the role of power electronics converter comes into action. Power electronics converter provides an intermediate role between the source of renewable energy and grid. The PWM inverter is more demanding nowadays which is used to convert the DC power obtained from different renewable energy sources to AC power but the quality of power is distorted leads to total harmonic distortion which is undesirable. In order to mitigate this problem, the multilevel inverter comes into handy as the THD is tremendously reduced in it.

The two factors have a prominent role in order to cope with problem of harmonics. Firstly, by means of power filters but it is cost demanding as it is made up of different kind of metals [1]. Secondly, the fundamental component of output waveform must be chopped off with several numbers of levels [1]. In case of three phase system, the alternate way to get away from the problem of harmonic is to switch only one phase per switching instant while the other two phases keep on their initial position.

The role of multilevel converters appears when total harmonic distortion (THD) has become a significant problem which needs to mitigate in order to transfer maximum amount of power.PWM (Pulse width modulation) is a technique through which the ON/OFF duration of the power switch (IGBT, MOSFET) can be controlled in an efficient manner by properly adjusting the width of the pulse. It has a prominent role in the speed control of motor, switch mode converters etc.

The inverter is divided into two categories i.e. VSI (voltage source inverter) and CSI (current source inverter). This thesis is concerned with the VSI so it is discussed in this section. As the name suggests, the VSI is fed from stiff DC voltage source and convert it into AC voltage with negligible amount of Thevenin impedance [2]. If the source is

not considered to be stiff, a large capacitor or a bank of capacitor is placed between the source and the inverter [2], [3]. This DC is obtained from battery bank by connecting several cells in series or parallel fashion or from different renewable sources. The nature of output voltage can be varied from constant voltage to a variable voltage depending upon the application ranging from Static VAR Generator (SVG) and compensator (SVC), uninterruptable power supply (UPS) and AC motor drives [2]. The output voltage produced by VSI is independent of the load.

Several types of multilevel converter have been proposed according the topological structures which includes Diode clamped multilevel converter (DCMC), flying capacitor multilevel converter (FCMC) and cascaded H-bridges. The other names are also proposed for these topologies. DCMC is also regarded as Neutral point converter (NPC). In the same fashion FCMC is also regarded as capacitor clamped converter (CCC). DCMC is getting more popularity in industrial point of view therefore this thesis has main focused on DCMC. The name multilevel converter is regarded for those converters whose output carries more than 2 DC levels. Here, the phase voltages contain 3 different DC levels so it is regarded as 3-level inverter.

The SVPWM (space vector pulse width modulation) is categorized in two ways i.e. two level and multilevel converter. Multilevel inverter has more advantages over two level inverter but difficult to implement due to large number of switching vectors. By comparative analysis between the 2-level and 3-level inverter, 3-level has more power switches i.e.12 and space vector diagram contain 27 switching vectors rather than 8 causes a less harmonic distortion. In case of 2-level inverter, the worst case error between the applied voltage and desired voltage is quite high as compared to multi-level inverter. As a result of this action the harmonics profile of 3-level inverter is much better than 2-level inverter which leads to provide better waveform quality. Fig.1 represents the worst error exist between these two kinds of inverter. In case of 2-level inverter, the desired voltage is 0.25 V_{DC} while the applied potentials are $+0.5V_{DC}$ and $-0.5V_{DC}$. The duration of $+0.5V_{DC}$ is greater than $-0.5V_{DC}$. In case of 3-level inverter, the desired voltage is same while the applied potentials are $+0.5V_{DC}$ and $0V_{DC}$ and having same duration of being remain in conduction mode.

The challenging task is to calculate the duty cycle of each power switch [11]. The more the level of the inverter the more the number of vectors to switch leads to provide better quality of output in terms of harmonics and amplitude.
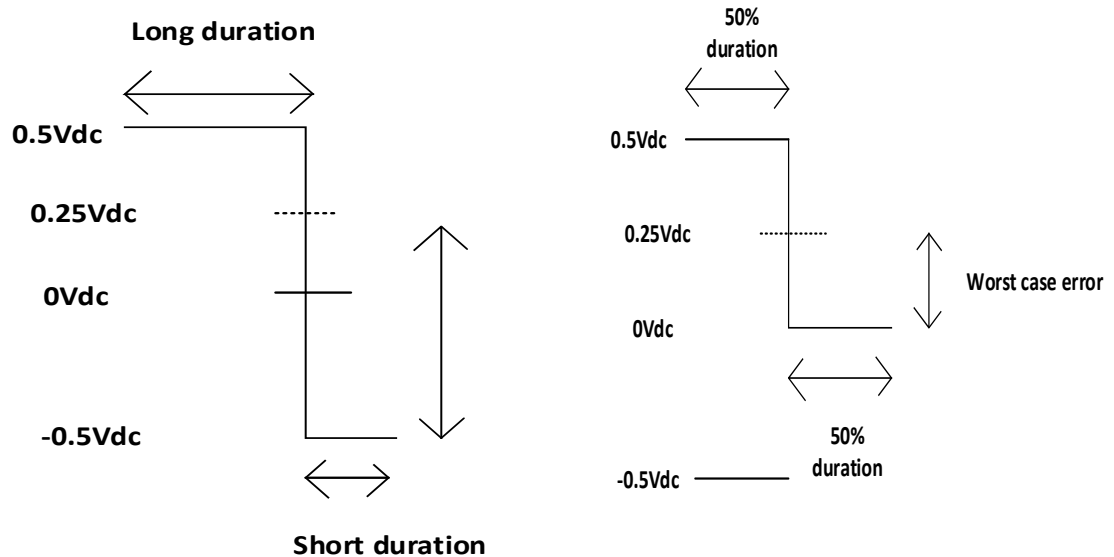
Fig.1 Worst error representation of 2-level and 3-level inverter

1.2 Thesis Outline

This thesis contains the 5 basic chapters. It begins with the introduction chapter which contains the objective of the thesis and the need of three-level SVPWM. It also presents the small introduction of VSI and the glimpse of comparison between two-level and three-level inverter.

Chapter 2 has given the brief concept of different modulation strategies used in multilevel inverter through which the duty cycle of the power switches can be controlled in an efficient manner. The purpose of different modulation schemes is to reduce the higher order harmonics and getting higher amplitude of fundamental component.

Chapter 3 presents the theory, concept and background of three-level SVPWM. The concept of voltage source inverter (VSI) along with background of NPC inverter has been developed. The derivation of pole voltages will be done based on the selection of particular sector and region. Vector switching times is also calculated along with duty ratio of power switches. The role of redundant vectors to control the DC midpoint potential control is also discussed.

In chapter 4 the simulation model for the SVPWM is designed on the basis of theory discussed in the previous chapters. The output of region and sector selection, line to line voltage and each phase voltage before and after incorporating the filter will be explained. The harmonic analysis at each output stage is also incorporated.

The main conclusion drawn from the simulation and future work proposal will be discussed in chapter 5.

2. MODULATION STRATEGIES

2.1 Modulation Techniques for Multilevel inverter

The purpose of modulation is to control the duration of power switches to achieve the switching pattern by means of desired amplitude and frequency. The two common modulation techniques available to get the gating signal sequence are carrier based modulation and space vector modulation. This thesis is more focused on the later one while the principle of carrier based modulation is defined a bit for comparison among the two.

2.1.1 Carrier based modulation

In carrier based PWM, gating pulses are obtained by comparison between a high frequency triangular carrier signal with a low frequency modulated signal. It is further divided into two schemes i.e. two-level shifted carriers and phase shifting of level shifted carriers for three level inverters. There is a general rule of thumb for this particular modulation scheme, if the converter is designed for 'n' number of voltage levels than 'n-1' number of triangular carriers [3] required to get the gating signal by comparing the modulating signal with these carriers.

2.1.1.1 Two-level shifted carriers

In three level inverter there is two pair of complimentary switches so it need two high frequency carriers operating at the same frequency and amplitude but they are level shifted by means of amplitude. Fig.2, shows the three modulating signal compared with two triangular carriers. One carrier is running between 0V and 1V while the other carrier is running between 0V and -1V, both carriers have same amplitude and frequency.

Switching logic

For simplicity, the upper carrier is regarded as carrier 1 while the bottom carrier is regarded as carrier 2. R-phase is plotted in black, Y-phase in red while B-phase in blue.

Considering the R-phase only,

When R-phase> carrier 1 and R-phase> carrier 2 yields $0.5V_{DC}$ pole voltage.
When R-phase< carrier 1 and R-phase< carrier 2 yields $-0.5V_{DC}$ pole voltage.

When R-phase> carrier 1 and R-phase< carrier 2 yields $0V_{DC}$ pole voltage.

Same is applied for Y and B phase.
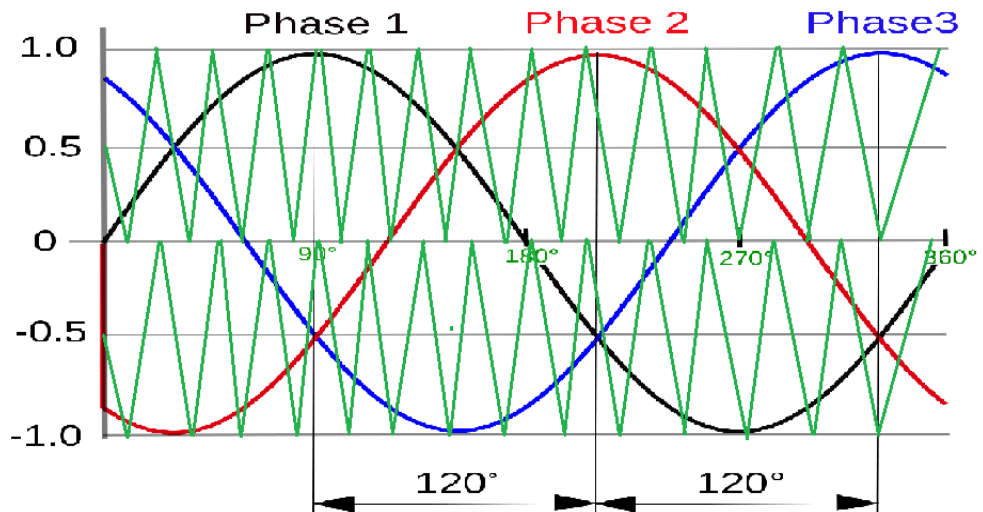
Figure 2 Level shifted carriers

2.1.1.2   Phase shifting of level shifted carriers

In this modulation scheme two high frequency carriers of same amplitude and frequency but displaced by some angle 'Θ'. Fig.3. shows two carriers, the top carrier is remained on its position while the bottom carrier drawn with brown line is displaced by certain amount of angle. This leads to provide same fundamental component but it creates more THD. The switching scheme will remain same as voltage shifted carriers.
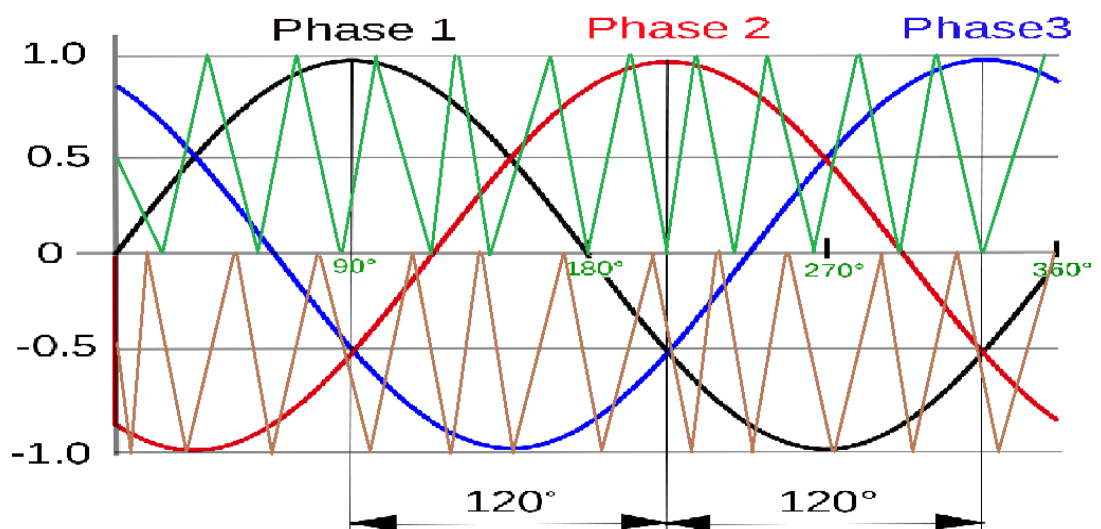
Figure 3 Phase shifted carriers
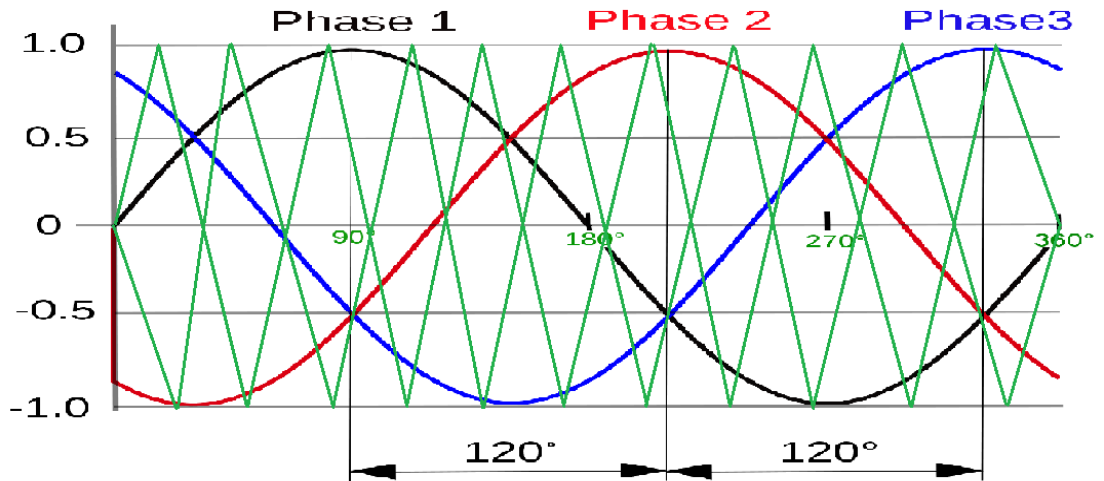
Figure 4 Out of phase shifted carriers

Fig.5 shows the switching sequence of two out of phase shifted carriers diagrammatically. Here, mR, mY and mB are the three modulating signal. 1, 0 and -1 are the three conditions of power switches of NPC.

1= Top two switches are ON in each phase causes $0.5V_{DC}$ at the pole.

0= Middle two switches are ON in each phase causes $0V_{DC}$ at pole.

-1= Bottom two switches are ON in each phase causes $-0.5V_{DC}$ at pole.

R	+	+	+	0
Y	-	0	0	0
B	-	-	-	0
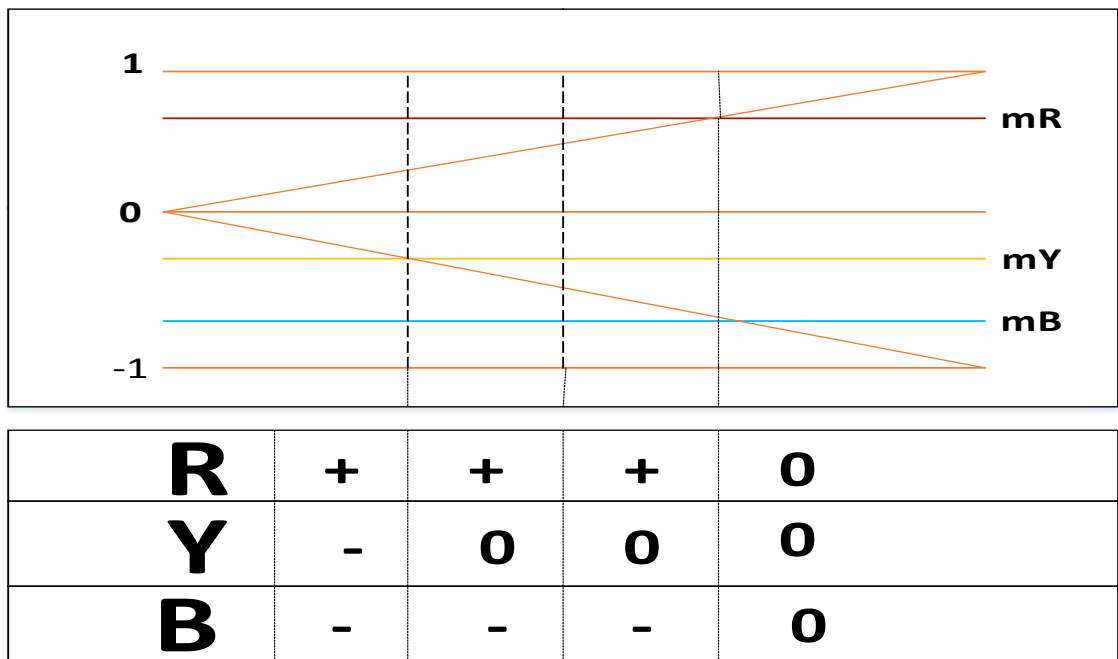
Figure 5 Switching sequence of out of phase carrier

2.1.2 Space Vector Modulation

Space vector modulation (SVM) is a modulation technique used to create PWM pulses. It is more extensive and computational technique among the industrial drive application [4]. It is more demanding due to easier digital implementation on DSP controller [9] and provides better conversion of DC into AC. It comprises of different switching vectors with different magnitude and angle. Each switching state defines the different output state which is obtained by combination of different stationary vector. SVM is based on the conversion of three phase quantities to 2-dimensional plane. A plane has always two-coordinate system. The name stationary reveals from the fact that it is remained in stationary position in space. The bunch of these vectors combine together to form space vector diagram. It indicates the position of each vector in space with respect to its magnitude and angle and the reference vector rotates with constant switching frequency within the hexagon. At each switching instant some mathematical calculations were performed to get the PWM pulses. When the reference vector rotate within the hexagon the inverter will operate in under modulation region or linear provide a smooth waveform at the output terminal. In this region the inverter transfer characteristics are naturally linear [2]. The over modulation region or non-linear region occur when the reference vector outside the premises of hexagon.

The space vector diagram for a three level inverter is shown below,
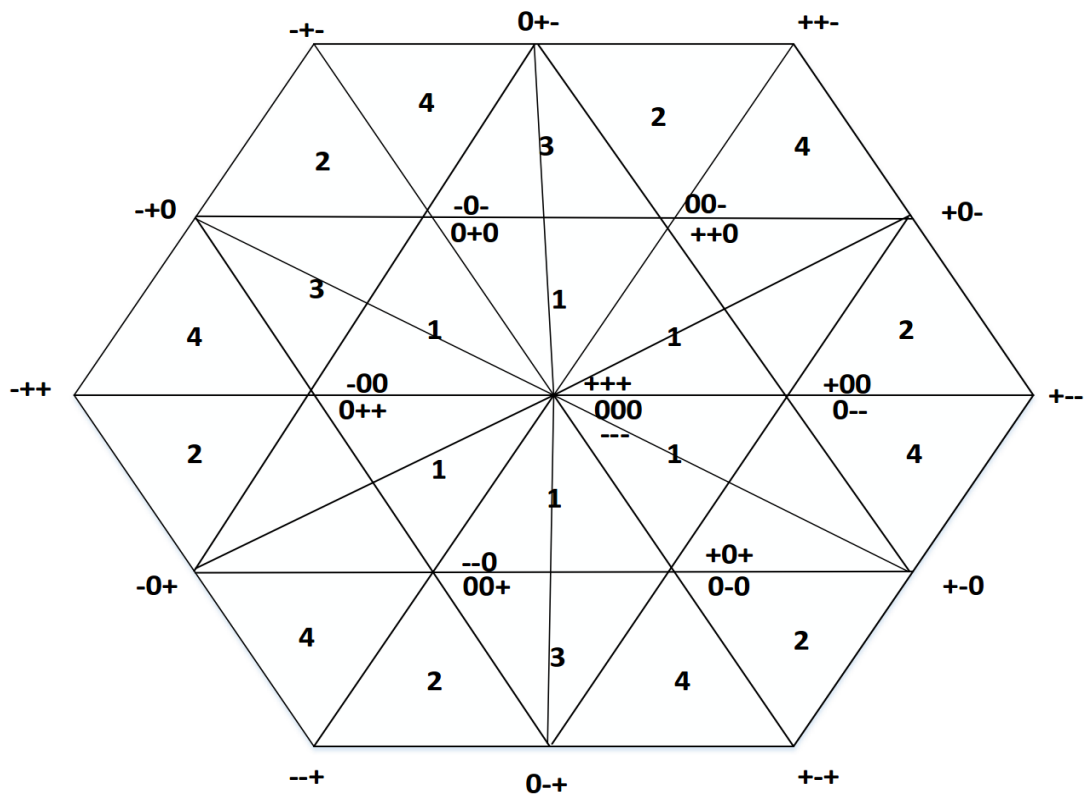
Figure 6 Space vector diagram for three-level inverter

Features of SVM

- Less harmonic distortion causes a minimal switching loss.
- Easy to implement on DSP controllers and microprocessor [8].
- Proper DC bus utilization [9].
- Required complex mathematical calculation.

2.2 Conclusion

In order to connect the output produce by the converter to the electric grid, it must be synchronized with the grid properties such as frequency, phase and amplitude. These properties must closely resemble to the sinusoidal wave. To get this kind of wave obtained from separate DC source, the inverter must be incorporated between the DC source and electric grid. The switches must be ON/OFF in a predefined manner which can be done by different modulation strategies. Here in this chapter different modulation strategies have been discussed. By comparative analysis between these two modulation strategies, SVPWM carries approximately 15% better utilization of voltages [22]. The overview of sine pulse width modulation (SPWM) has given just only for reference while the concept behind the SVPWM is further discussed in detail in the next two chapters.

3. ANALYSIS OF THREE LEVEL INVERTER

3.1 Introduction

The term "space" comes from the fact that it is composed of two dimensional plane i.e. real plane 'α' and imaginary plane 'β'. In order to avoid more complex calculation of three phase system, the three phase quantities are transformed to two phase quantities using Clark's transformation.

3.2 Concept of Space Vector

The concept of space vector emerged from the theory of three phase electrical machines i.e. induction machines and synchronous machines. All of these machines comes up with a three set of stator windings with each winding is separated from each other by an angle of 120°. When these windings are connected to three phase AC source produces a magnetic flux. This associated flux causes a production of magnetomotive force (mmf) when ampere-turns setup by magnetic flux which rotate in the air gap with certain angular frequency 'ω'. When this flux is linked with rotor bars causes a rotor to rotate with synchronous speed 'N_S'. This revolving mmf is an example of space vector.

Mathematically the pulsating magnetic field produced by a single phase winding,

$$F_{R,1} = Ki_R \, Cos(\theta_{ae}) \tag{1}$$

where,

F= mmf produced in the air-gap

i_R = rotor current

1 = fundamental component of revolving mmf

θ_{ae}= angle between the produced magnetic field with respect to its axis.

Since this current is sinusoidal in nature as it is taking from AC source. So,

$$i_R = I_m \, Cos(\omega t) \tag{2}$$

By substituting eq. (2) in eq. (1) we get,

$$F_{R,1} = KI_m \, \mathrm{Cos}(\theta_{ae}) \mathrm{Cos}(\omega t)$$

By applying product rule of cosine function gives,

$$F_{R,1} = \frac{KI_m}{2} \left[\mathrm{Cos}\left(\theta_{ae} - \omega t\right) + \mathrm{Cos}\left(\theta_{ae} + \omega t\right) \right] \tag{3}$$

From the above equation it can easily be deduced that the pulsating magnetic field is resolved into components i.e. one rotates clockwise while the other rotates in anticlockwise direction.

Now extend this concept to a three phase winding. The three phase current can be written as,

$$i_R = I_m \, \mathrm{Cos}\left(\omega t\right) \qquad\qquad i_Y = I_m \, \mathrm{Cos}\left(\omega t - 120\right) \qquad\qquad i_B = I_m \, \mathrm{Cos}\left(\omega t + 120\right)$$

$$I_{R,1} = Ki_R \, \mathrm{Cos}\left(\theta_{ae}\right)$$

Similarly,

$$I_{Y,1} = Ki_Y \, \mathrm{Cos}\left(\theta_{ae} - 120\right) \qquad\qquad\qquad\qquad I_{B,1} = Ki_B \, \mathrm{Cos}\left(\theta_{ae} + 120\right)$$

which than produce a m.m.f as given below,

$$F_{R,1} = Ki_R \, \mathrm{Cos}(\theta_{ae}) \tag{4}$$

$$F_{Y,1} = Ki_Y \, \mathrm{Cos}(\theta_{ae} - 120^o) \tag{5}$$

$$F_{B,1} = Ki_B \, \mathrm{Cos}(\theta_{ae} - 240^o) \tag{6}$$

By substituting the three phase current in above equation gives,

$$F_{R,1} = F_{max} \, \mathrm{Cos}(\theta_{ae}) \mathrm{Cos}(\omega t) \tag{7}$$

$$F_{Y,1} = F_{max} \, \mathrm{Cos}(\theta_{ae} - 120^o) \mathrm{Cos}(\omega t - 120^o) \tag{8}$$

$$F_{B,1} = F_{max} \, \mathrm{Cos}(\theta_{ae} - 240^o) \mathrm{Cos}(\omega t - 240^o) \tag{9}$$

where,

$$F_{max} = K * I_m$$

By using trigonometric identities the equation (7) to (9) gives,

$$F_{R,1} = \frac{F_{max}}{2}\left[\text{Cos}\left(\theta_{ae} - \omega t\right) + \text{Cos}\left(\theta_{ae} + \omega t\right)\right] \tag{10}$$

$$F_{Y,1} = \frac{F_{max}}{2}\left[\text{Cos}\left(\theta_{ae} - \omega t\right) + \text{Cos}\left(\theta_{ae} + \omega t - 240^o\right)\right]$$

Also can be written as,

$$F_{Y,1} = \frac{F_{max}}{2}\left[\text{Cos}\left(\theta_{ae} - \omega t\right) + \text{Cos}\left(\theta_{ae} + \omega t + 120^o\right)\right] \tag{11}$$

$$F_{B,1} = \frac{F_{max}}{2}\left[\text{Cos}\left(\theta_{ae} - \omega t\right) + \text{Cos}\left(\theta_{ae} + \omega t - 480^o\right)\right]$$

Also can be written as,

$$F_{B,1} = \frac{F_{max}}{2}\left[\text{Cos}\left(\theta_{ae} - \omega t\right) + \text{Cos}\left(\theta_{ae} + \omega t + 240^o\right)\right] \tag{12}$$

The average value can be computed as,

$$F_{ag,1} = \left(F_R^+ + F_Y^+ + F_B^+\right) + \left(F_R^- + F_Y^- + F_B^-\right)$$

From the above equation the vector which revolves in anti-clockwise direction gets cancelled gives,

$$F_{ag,1} = 3\frac{F_{max}}{2}\text{Cos}\left(\theta_{ae} - \omega t\right) \tag{13}$$

This is the vector which revolves in the air gap between stator and rotor with angular speed (ω).

3.3   Multilevel Voltage Source Inverter

3.3.1   Neutral-Point-Clamped Inverter

There is a variety of multilevel converters available like cascaded H-Bridge inverter, flying capacitor inverter. Each converter has its own advantage depending upon the application but neutral-point-clamped inverter has gained more popularity and attention as far as this thesis is concerned. If the output voltage level and power level of PWM increased, the devices need to be connected in series gives a formation of NPC inverter [10]. It is also named as "Diode Clamped multilevel inverter" because the diodes are used to clamped the potential at DC mid-point 'o' to the switching elements. A simple configuration of three levels NPC inverter is shown in Fig.7. In general, for n-level

converter requires (n-1) capacitors, 2(n-1) power switches per phase and 2(n-2) clamping diodes [19]. For a three level converter 4 power switches are required for a single phase. For a three phase system it comprises of 12 power switches i.e., IGBT's. The stiff DC link can be created by connecting the two capacitors in series. The mid-point of the two capacitors acts as a DC neutral point 'O' which is different from the load neutral point (N) connected in star connected load fashion. The diodes are known as clamped diodes which are used to clamp the power switches to DC neutral. Because of this kind of action the power switches is capable of carrying either $+\frac{Vdc}{2}$, $-\frac{Vdc}{2}$ or 0.
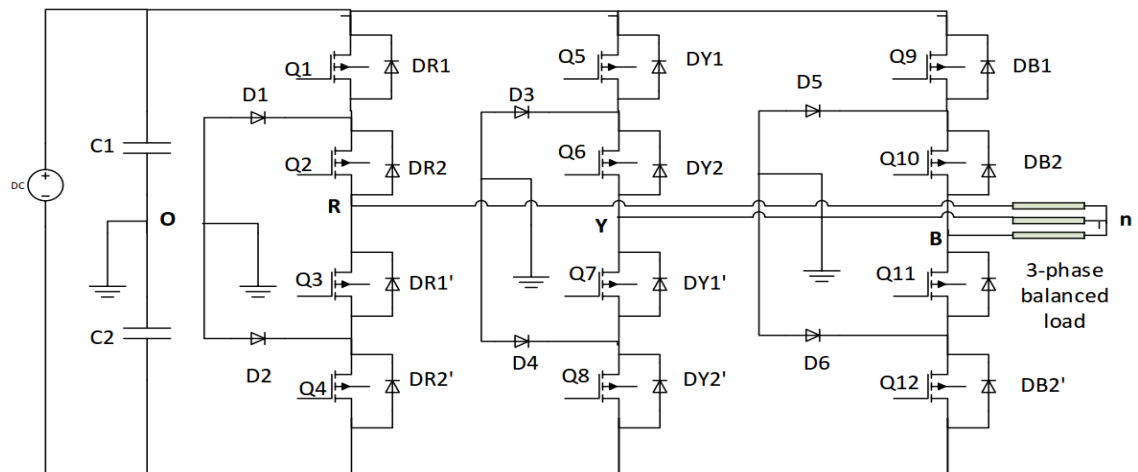
Figure 7 3-Level NPC inverter

The higher number of voltage levels can be achieved by the addition of these switching devices. The higher the number of levels the more smooth the waveform is which eliminates the harmonics causing a higher output at the load.

In order to get 0.5Vdc at the pole A the upper two switches (S_{A1} and S_{A2}) need to be conduct. On the contrary -0.5Vdc can be achieved by conducting bottom two switches (S_{A3} and S_{A4}). The middle two switches (S_{A2} and S_{A3}) connect the pole A to the neutral point "o" producing 0Vdc. S_{A1} and S_{A3} are connected in complimentary fashion i.e. S_{A1} and S_{A3} cannot conduct at the same the time. Similarly for S_{A2} and S_{A4}.

Table 1 3-Level NPC inverter output voltage levels and their switching states for phase A

Voltage Levels (V_{Ao})	Status of ON switches
+0.5V_{DC}	S_{A1} and S_{A2}
0V_{DC}	S_{A2} and S_{A3}
-0.5V_{DC}	S_{A3} and S_{A4}

3.4 SWITCHING STATES

In a three level inverter load neutral is different from DC mid-point 'o'. The phase voltage is measured from the pole of each leg to the DC mid-point 'o' while the line voltage is measured as the difference between two poles. The switching states represent the operating point of the power switch. For a three level inverter the switching state of each switch is represented as either '+', '0', '-'.
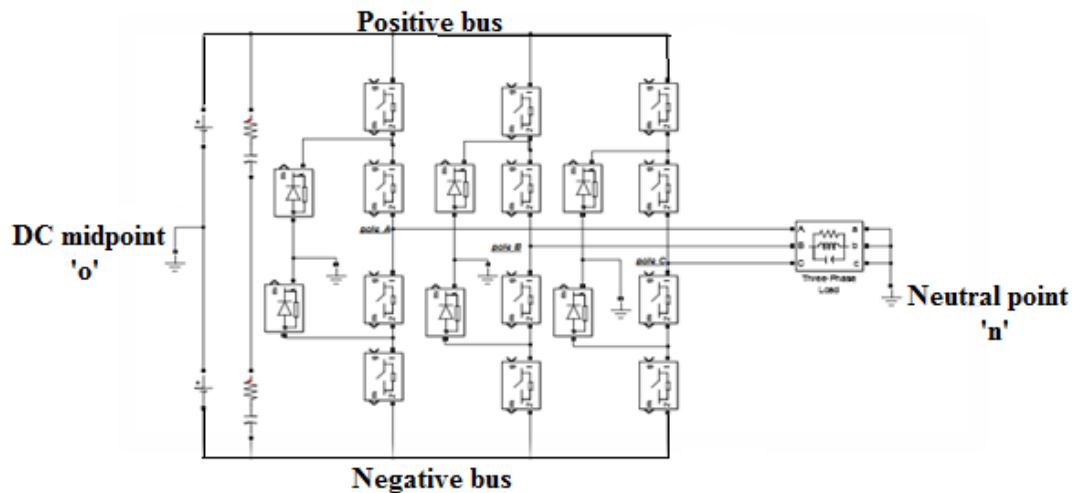
Figure 8 Neutral point and DC point representation

[+] State

During the operation of this state the upper two switches of each leg of the inverter are ON which makes the two clamping diodes are reverse biased for a certain duration of time causes positive DC bus voltage appears across the output of each pole while the two bottom switches are at OFF position.In this state the output is $\frac{V_{dc}}{2}$.

Figure 9 Switching state at [+]

[0] State

During the operation of this state the middle switches of each leg of the inverter is turned ON causes the clamping diodes forward biased makes a direct connection between the output to the DC midpoint 'o'. In this state the direction of current is dependent on the load. In this state the output is $0\ V_{dc}$.
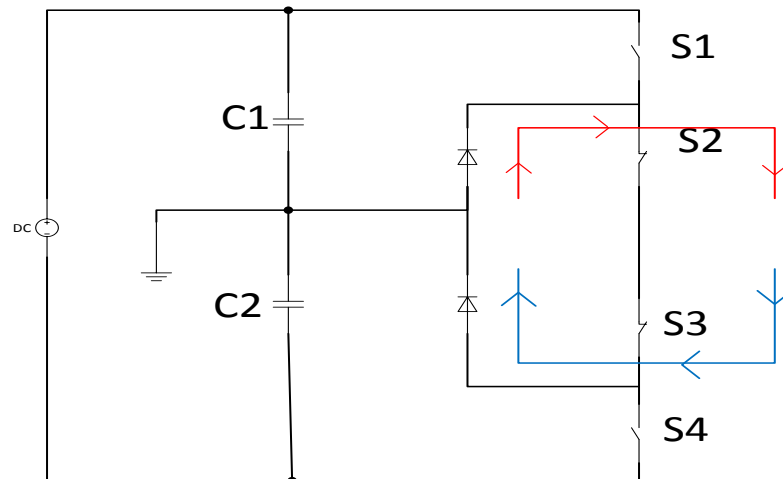
Figure 10 Switching state at [0]

[-] State

During the operation of this state the bottom two switches of each leg of the inverter are ON which makes the two clamping diodes are reverse biased for a certain duration of time causes negative DC bus voltage appears across the output of each pole while the two top switches are at OFF position.In this state the output is $-\frac{V_{dc}}{2}$.
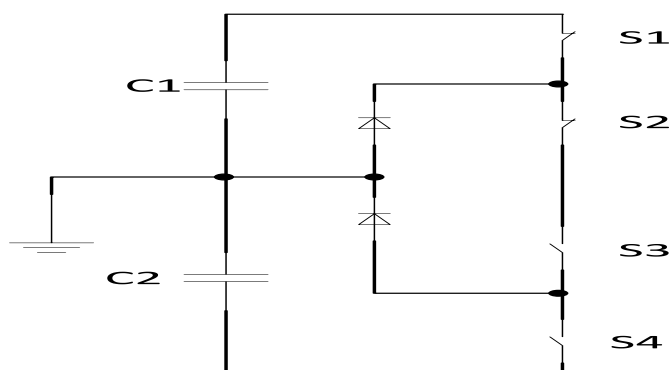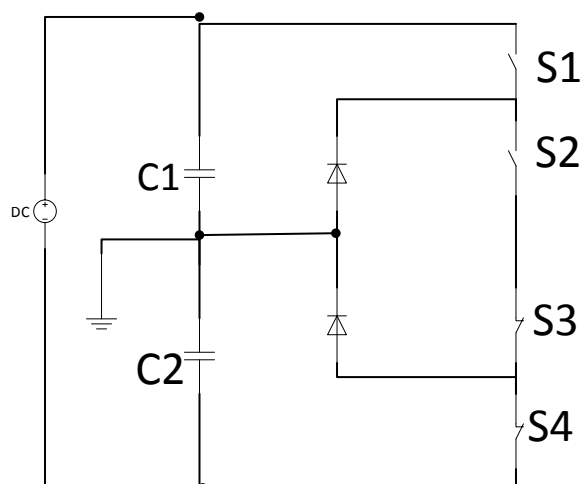

Figure 11 Switching state at [-]

Table 2 Status of power switches during switching states [16]

State	S1	S2	S3	S4	Pole Voltage
[+]	ON	ON	OFF	OFF	$\dfrac{V_{DC}}{2}$
[0]	OFF	ON	ON	OFF	$0V_{DC}$
[-]	OFF	OFF	ON	ON	$-\dfrac{V_{DC}}{2}$

3.5 SPACE VECTOR PWM ALGORITHM

This section describes the fundamental concept of space vector modulation which involves the mathematical calculation of V_α and V_β at different switching state, dwell time calculation of stationary vectors, criteria for the selection of region and sector and sequence of 7-segments, 9-segments and 13-segments switching vector scheme.

3.5.1 SPACE VECTOR TRANSFORMATION

The mmf produced in a three phase winding can also be produced by a two phase fictitious winding as well but these two winding should be separated in space by 90° apart.
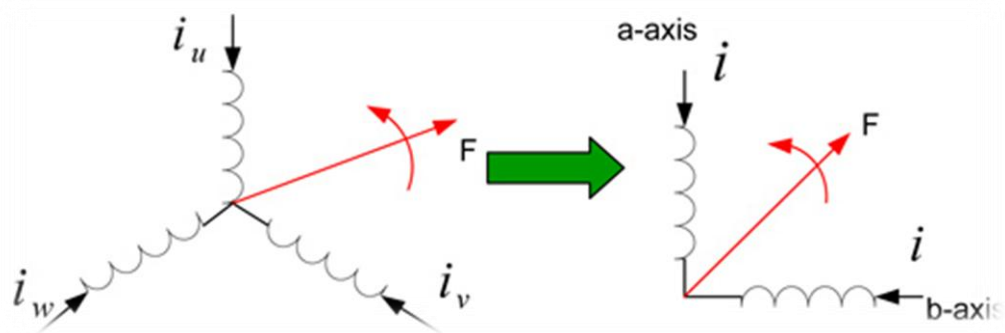
Figure 12 Pictorial view of Clark's transformation [5]

Resolve the three phase quantities 'R','Y' and 'B' into equivalent two phase components as follows,

$$Ni_\alpha = Ni_R + Ni_Y \cos 120^o + Ni_B \cos 240^o$$
$$Ni_\beta = Ni_Y \cos 30^o + Ni_B \cos 150^o$$

There is no component of R-phase in the direction of 'β' axis.

By cancelling the common terms in above two equations gives,

$$i_\alpha = i_R + i_Y \cos 120^o + i_B \cos 240^o \qquad \rightarrow \qquad i_\alpha = i_R - \frac{i_Y}{2} + \frac{i_B}{2}$$

$$i_\alpha = i_R - \frac{1}{2}(i_Y + i_B) \tag{14}$$

By applying Kirchhoff current law,

$$i_R + i_Y + i_B = 0$$

$$i_\alpha = i_R - \frac{1}{2}(-i_R) \qquad \rightarrow \qquad i_\alpha = \frac{3}{2}(i_R) \tag{15}$$

$$i_\beta = i_Y \cos\left(30^o\right) + i_B \cos\left(150^o\right) \qquad \rightarrow \qquad i_\beta = \frac{\sqrt{3}}{2}(i_Y - i_B) \tag{16}$$

The eq. (15) and eq. (16) can also written in matrix form,

$$\begin{bmatrix} i_\alpha \\ i_\beta \end{bmatrix} = \begin{bmatrix} \frac{3}{2} & 0 & 0 \\ 0 & \frac{\sqrt{3}}{2} & \frac{-\sqrt{3}}{2} \end{bmatrix} \begin{bmatrix} i_R \\ i_Y \\ i_B \end{bmatrix}$$

For a 3-φ balanced star connected load,

$$\begin{bmatrix} V_\alpha \\ V_\beta \end{bmatrix} = \begin{bmatrix} \frac{3}{2} & 0 & 0 \\ 0 & \frac{\sqrt{3}}{2} & \frac{-\sqrt{3}}{2} \end{bmatrix} \begin{bmatrix} V_R \\ V_Y \\ V_B \end{bmatrix}$$

The magnitude of the reference vector can be calculated by,

$$V_{ref} = \sqrt{V_\alpha{}^2 + V_\beta{}^2}$$

The direction of the reference vector can be computed as,

$$\Theta = tan^{-1}\left(\frac{V_\beta}{V_\alpha}\right)$$

3.5.2 Calculation of position of vectors with respect to its magnitude and direction on space vector plane

Since $V_{RO(avg)}$, $V_{YO(avg)}$, $V_{BO(avg)}$ are available in sinusoidal quantities so they can easily represent in phasor form. The 3-phase voltages and their corresponding line-line voltages are given in Fig.13.
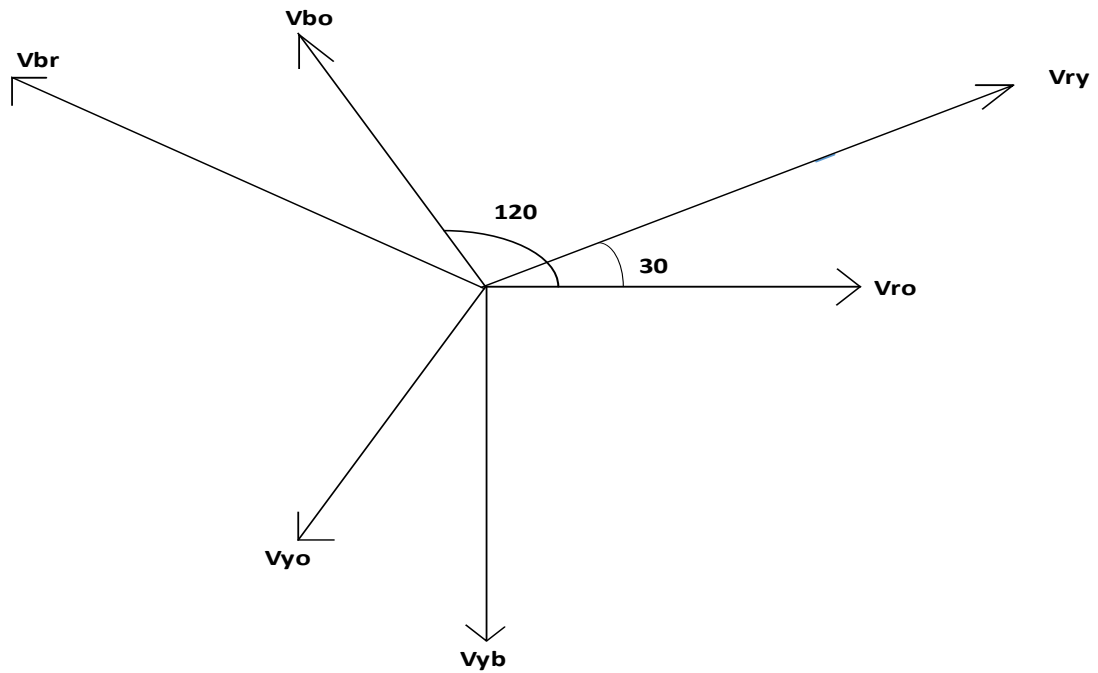
Figure 13 Phasor-representation of phase and line-line voltages

For instance consider the switching state [+--] which means the two top switches of R-leg are turned ON and the bottom two switches of Y-leg & B-leg are turned ON.

For 3-φ star connected balance load,

$$V_{RN} = \frac{V_{RY} - V_{BR}}{3}$$

where,

$$V_{RY} = V_{RO} - V_{YO}$$

$$V_{RY} = \frac{V_{DC}}{2} - \left(-\frac{V_{DC}}{2}\right) \quad \rightarrow \quad V_{RY} = V_{DC}$$

$$V_{BR} = V_{BO} - V_{RO}$$

$$V_{BR} = \frac{-V_{DC}}{2} - \left(\frac{V_{DC}}{2}\right) \quad \rightarrow \quad V_{BR} = -V_{DC}$$

$$V_{RN} = \frac{V_{DC} + V_{DC}}{3} \quad \rightarrow \quad V_{RN} = \frac{2V_{DC}}{3}$$

$$V_{\alpha} = \frac{3}{2} V_{RN} \text{ which gives us,}$$

$$V_\alpha = V_{DC} \tag{17}$$

$$V_\beta = \frac{\sqrt{3}}{2}(V_{YN} - V_{BN})$$

$$V_{YN} = \frac{V_{YB} - V_{RY}}{3}$$

$$V_{YN} = \frac{-1}{3}V_{DC} \text{ and } V_{BN} = \frac{-1}{3}V_{DC}$$

$$V_\beta = 0 \tag{18}$$

The magnitude of stationary vector become,

$$V_{ref} = \sqrt{V_{DC}{}^2 + 0} \qquad \rightarrow \qquad V_{ref} = V_{DC}$$

The direction of stationary vector becomes,

$$\Theta = tan^{-1}\left(\frac{0}{V_{DC}}\right) \rightarrow \Theta = 0^o$$

which constitutes a vectorV_5 in space vector plane. The corresponding 27 vectors are formed in the same way.

- 6 vectors out of 27 vectors having same magnitude of V_{DC} with 60° degrees apart. These vectors are V_5 [+--], V_9 [++-], V_{11} [-+-], V_{17} [-++], V_{21} [--+] andV_{25} [+-+].

- 12 vectors out of 27 vectors are having a same magnitude of $\frac{V_{DC}}{2}$ and each two vectors are placed at 60° degrees apart. These vectors include V_3 [+00] and V_4 [0--], V_7 [++0] and V_8 [00-], V_{12} [010] and V_{13} [-0-], V_{14} [0++] and V_{15} [-00], V_{19} [00+] and V_{20} [- -0], V_{23} [+0+] and V_{24} [0-0].

- 6 vectors out of 27 vectors having same magnitude of $\frac{\sqrt{3}}{2}V_{DC}$ with 60° degrees apart but first vector lies at 30°. These vectors are V_6 [+0-], V_{10} [0+-], V_{16} [-+0], V_{18} [-0+], V_{22} [0-+] andV_{26} [+-0].

- The remaining 3 vectors are known as zero vectors having amplitude of 0 V_{DC} and an angle 0^0.

3.5.3 Classification of Stationary Vectors

The three level SVPWM composed of 27 stationary vectors (V_1-V_{27}). They are further classified into four groups on the basis of their magnitude. The zero vectors corresponds to those vectors whose magnitude is $0V_{DC}$. These small vectors having an amplitude of $\frac{1}{2}V_{DC}$. For medium vectors the amplitude is $\frac{\sqrt{3}}{2}V_{DC}$. The last group of stationary vectors is known as large vectors whose amplitude is V_{DC}. These group combine together to form space vectors as shown in fig.14. Table 3 represents the classification of vectors with its amplitude.
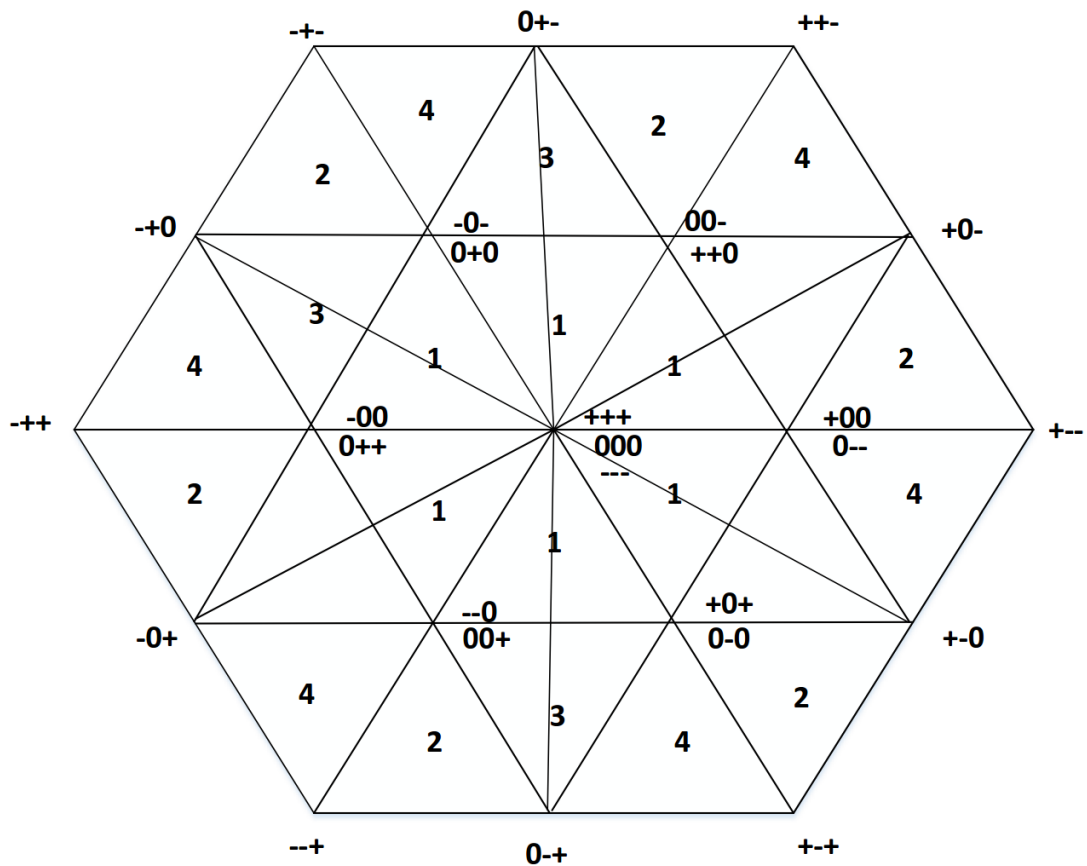
Figure 14 Space vector of three level NPC

Table 3 Switching schemes of stationary vectors

Vector	Switching State	Vector Classification	Magnitude
V_1	000	Zero Vector	$0\,V_{DC}$
V_2	---	Zero Vector	$0\,V_{DC}$

V_3	+00	Small Vector	$\frac{1}{2} V_{DC}$
V_4	0-	Small Vector	$\frac{1}{2} V_{DC}$
V_5	+--	Large Vector	V_{DC}
V_6	+0-	Medium Vector	$\frac{\sqrt{3}}{2} V_{DC}$
V_7	++0	Small Vector	$\frac{1}{2} V_{DC}$
V_8	00-	Small Vector	$\frac{1}{2} V_{DC}$
V_9	++-	Large Vector	V_{DC}
V_{10}	0+-	Medium Vector	$\frac{\sqrt{3}}{2} V_{DC}$
V_{11}	-+-	Large Vector	V_{DC}
V_{12}	0+0	Small Vector	$\frac{1}{2} V_{DC}$
V_{13}	-0-	Small Vector	$\frac{1}{2} V_{DC}$
V_{14}	0++	Small Vector	$\frac{1}{2} V_{DC}$
V_{15}	-00	Small Vector	$\frac{1}{2} V_{DC}$
V_{16}	-+0	Medium Vector	$\frac{\sqrt{3}}{2} V_{DC}$
V_{17}	-++	Large Vector	V_{DC}
V_{18}	-0+	Medium Vector	$\frac{\sqrt{3}}{2} V_{DC}$
V_{19}	00+	Small Vector	$\frac{1}{2} V_{DC}$
V_{20}	--0	Small Vector	$\frac{1}{2} V_{DC}$

V_{21}	--+	Large Vector	V_{DC}
V_{22}	0-+	Medium Vector	$\frac{\sqrt{3}}{2} V_{DC}$
V_{23}	+0+	Small Vector	$\frac{1}{2} V_{DC}$
V_{24}	0-0	Small Vector	$\frac{1}{2} V_{DC}$
V_{25}	+-+	Large Vector	V_{DC}
V_{26}	+-0	Medium Vector	$\frac{\sqrt{3}}{2} V_{DC}$
V_{27}	+++	Zero Vector	$0 V_{DC}$

Furthermore, these groups of vector fall in two groups of state i.e. **active state and null state.**

The null state corresponds to the condition when there is no power flow take place from DC side to AC side. In this state (I_{DC}=0A). It is also known as zero state and corresponding vectors are known as zero vectors. The zero vector group lie in this state. Whereas, active state is a state at which there is a transfer of power takes place between DC side and AC side and corresponding vectors are known as active vectors. Large vectors, medium vectors and small vectors are a part of this state.

3.5.4 Sectors selection

The space vector of three level inverter is divided into 6 sectors. Each sector comprise of 60° which makes the reference vector (V_{ref}) to rotate around 360°. Each sector is further divided into 4 regions. So, the space vector plane is split into 6*4=24 regions. The sector is classified on the basis of angle.

- $0^o \leq \Theta < 60^o$ reference vector (V_{ref}) lies in Sector 1.
- $60^o \leq \Theta < 120^o$ reference vector (V_{ref}) lies in Sector 2.
- $120^o \leq \Theta < 180^o$ reference vector (V_{ref}) lies in Sector 3.
- $180^o \leq \Theta < 240^o$ reference vector (V_{ref}) lies in Sector 4.
- $240^o \leq \Theta < 300^o$ reference vector (V_{ref}) lies in Sector 5.
- $300^o \leq \Theta < 360^o$ reference vector (V_{ref}) lies in Sector 6.
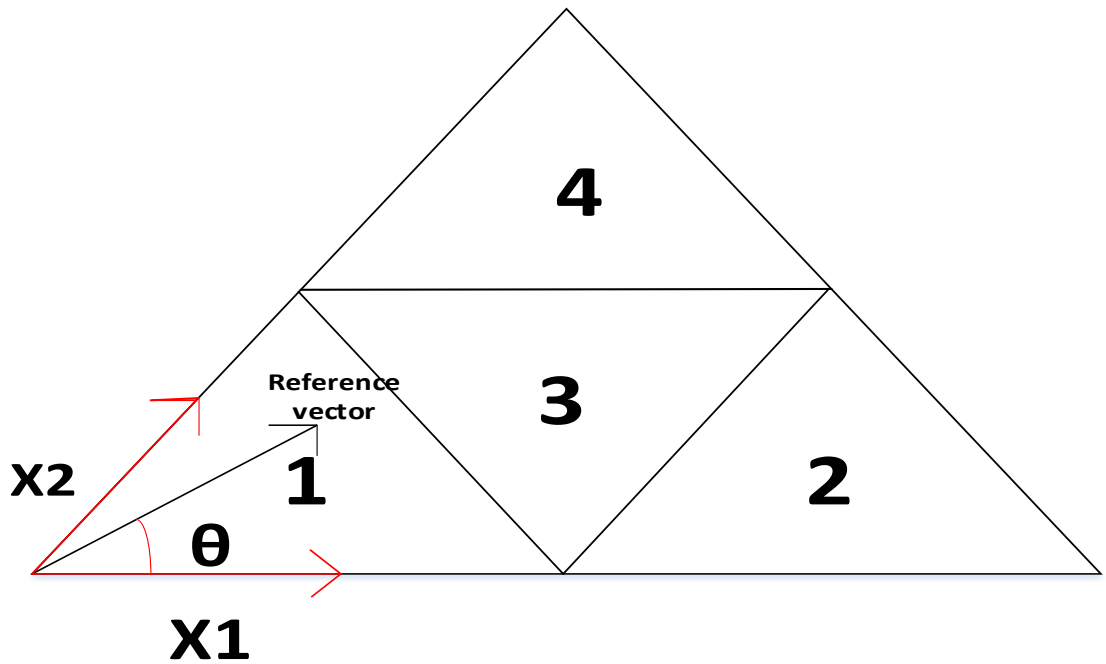
Figure 15 Sector I and all its four region

3.5.5 Methodology for region selection

The region selection is done by splitting the reference vector (V_{ref}) into its coordinates i.e. α and β.

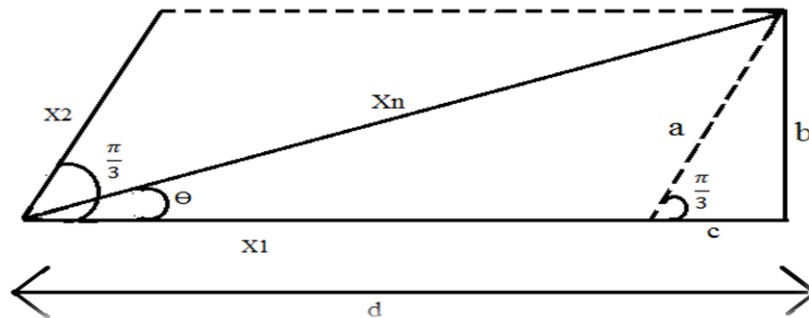*Figure 16 View of sector I, region I*

Calculation of X_2

$$Sin\left(\frac{\pi}{3}\right) = \left(\frac{b}{a}\right) \qquad \rightarrow \qquad a = \frac{b}{Sin\left(\frac{\pi}{3}\right)}$$

From fig.16, $b = X_n \, Sin\, \theta$ and $a = X_2$

$$X_2 = \frac{X_n \sin\theta}{\sin\left(\dfrac{\pi}{3}\right)} \qquad \rightarrow \qquad X_2 = \frac{2}{\sqrt{3}} X_n \sin\theta$$

Calculation of X_1:

$$d = X_1 + c$$

or $\ X_n \cos\theta = X_1 + c$

or $\ X_1 = X_n \cos\theta - c$ (19)

$$\cos\left(\frac{\pi}{3}\right) = \frac{c}{a} \qquad \rightarrow \qquad c = a\left(\frac{1}{2}\right)$$

From the above fig. a= X_2

$$c = \frac{2}{\sqrt{3}} X_n \sin\theta\left(\frac{1}{2}\right) \quad \rightarrow \quad c = \frac{X_n \sin\theta}{\sqrt{3}}$$ (20)

After putting eq. (20) in eq. (19)

$$X_1 = X_n \cos\theta - \frac{X_n \sin\theta}{\sqrt{3}} \qquad \rightarrow \qquad X_1 = X_n\left(\cos\theta - \frac{\sin\theta}{\sqrt{3}}\right)$$

- If $X_1 < 0.5 V_{DC}$, $X_2 < 0.5 V_{DC}$ and $(X_1 + X_2) < 0.5 V_{DC}$ the reference vector lies in region I.
- If $X_1 > 0.5 V_{DC}$ the reference vector lies in region II.
- If $X_1 < 0.5 V_{DC}$, $X_2 < 0.5 V_{DC}$ and $(X_1 + X_2) > 0.5 V_{DC}$ the reference vector lies in region III.
- If $X_2 > 0.5 V_{DC}$ the reference vector lies in region IV.

3.5.6 Dwell time calculation

This section describes the concept of dwell time calculation of the three nearest vector in any region by applying the simple concept of volt-second balance which states that **"the sum of the product of voltages of space vector and duration for which these voltages applied must equal to the product of reference voltage (V_{ref}) and sampling time (Ts)"**. It simply means for how much time the active vectors gets conduct. The sampling time for each switching state is 'Ts' second and each region is split into 'Ta', 'Tb' and 'Tc' second which is the time taken by stationary vectors to remain conduct for that duration.
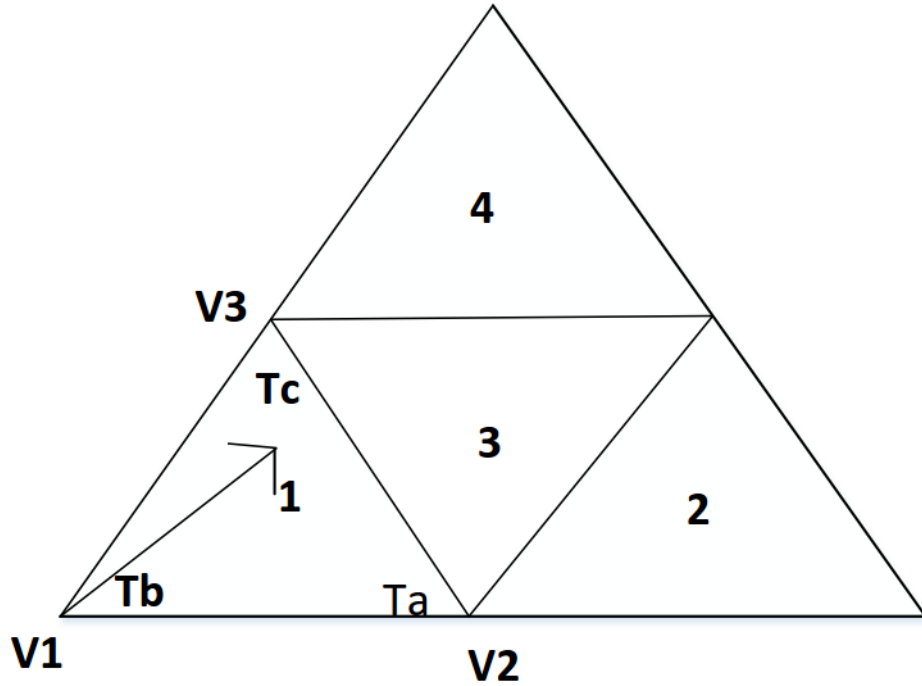
Figure 17 Active vectors and their corresponding time in sector I, region I

Apply volt-second balance in region I gives,

$$V_2 * T_a + V_1 * T_b + V_3 * T_c = V_{ref} * T_s \tag{21}$$

where,

$$V_1 = 0V_{DC}e^{j0} \qquad V_2 = \frac{1}{3}V_{DC}e^{j0} \qquad V_3 = \frac{1}{3}V_{DC}e^{j\frac{\pi}{3}}$$

The above equation becomes,

$$\frac{1}{3}V_{DC}e^{j0} * T_a + 0V_{DC}e^{j0} * T_b + \frac{1}{3}V_{DC}e^{j\frac{\pi}{3}} * T_c = V_{ref}e^{j\theta} * T_s$$

$$\frac{1}{3}V_{DC}\left(\text{Cos}\,0 + j\,\text{Sin}\,0\right)T_a + \frac{1}{3}V_{DC}\left(\text{Cos}\,\frac{\pi}{3} + j\,\text{Sin}\,\frac{\pi}{3}\right)T_c = V_{ref}\left(\text{Cos}\,\theta + j\,\text{Sin}\,\theta\right)T_s$$

Resolve into real and imaginary components,

$$\frac{1}{3}T_a + 0T_b + \frac{1}{6}T_c = \frac{V_{ref}}{V_{DC}}\text{Cos}\,\theta T_s \tag{22}$$

$$0T_a + 0T_b + \frac{\sqrt{3}}{6}T_c = \frac{V_{ref}}{V_{DC}}\text{Sin}\,\theta T_s \tag{23}$$

$$T_a + T_b + T_c = T_s \tag{24}$$

From eq. (23),

$$T_c = \frac{\sqrt{3}}{\sqrt{3}}\left(\frac{6}{\sqrt{3}}\frac{V_{ref}}{V_{DC}}\mathrm{Sin}\,\theta T_s\right) \qquad \longrightarrow \qquad T_c = 2m_a\,\mathrm{Sin}\,\theta T_s$$

where,

m_a= modulation index =

By substituting value of Tc in eq. (22) gives,

$$T_a = 3\frac{V_{ref}}{V_{DC}}\mathrm{Cos}\,\theta T_s - \frac{3}{\sqrt{3}}\frac{V_{ref}}{V_{DC}}\mathrm{Sin}\,\theta T_s$$

$$T_a = T_s\left[2m\,\mathrm{Sin}\left(\frac{\pi}{3}-\theta\right)\right]$$

By substituting values of Ta and Tc in eq. (24) gives,

$$T_b = T_s\left[1 - 2m\,\mathrm{Sin}\left(\frac{\pi}{3}+\theta\right)\right]$$

Here are the derived values of dwell times of sector I and region I for Θ varies from 0 to $\frac{\pi}{3}$.

The dwell time calculation for the remaining sectors and their corresponding region is done in the same way.

Table 4 Dwell time for sector I

Region	Ta	Tb	Tc
1	$\mathrm{Ts}\left[2m\sin\left(\frac{\pi}{3}-\theta\right)\right]$	$\mathrm{Ts}\left[1-2m\sin\left(\frac{\pi}{3}+\theta\right)\right]$	$2m\sin\theta\mathrm{T_s}$
2	$\mathrm{Ts}\left[2-2m\sin\left(\frac{\pi}{3}+\theta\right)\right]$	$2m\sin\theta\mathrm{T_s}$	$\mathrm{Ts}\left[2m\sin\left(\frac{\pi}{3}-\theta\right)-1\right]$
3	$(1-2m\sin\theta)\mathrm{T_s}$	$\mathrm{Ts}\left[2m\sin\left(\frac{\pi}{3}+\theta\right)-1\right]$	$\mathrm{Ts}\left[1-2m\sin\left(\frac{\pi}{3}-\theta\right)\right]$

| 4 | $2m(\sin\theta - 1)T_s$ | $Ts\left[2m\sin\left(\frac{\pi}{3} - \theta\right)\right]$ | $Ts\left[2 - 2m\sin\left(\frac{\pi}{3} + \theta\right)\right]$ |

The dwell time calculation for sector II to sector VI is also achieved by shifting these sectors to sector I. Since each sector is last long for $\frac{\pi}{3}$ radian and resulted angle is achieved by subtracting the multiple of $\frac{\pi}{3}$ from calculated angular displacement 'Θ' [6].

3.6 DC Neutral Point Potential Control

The whole space vector diagram is split into 4 different groups of vectors, they are classified as Large vectors (+--, ++-, -+-, -++, --+, +-+), Zero vectors (+++, ---, 000), Small vectors (+00, 0--, 00-, ++0, -0-, 0+0, -00, 0++, --0, 00+, +0+, 0-0) and Medium vectors (+0-, 0+-, -+0, -0+, 0-+, +-0). In large vectors the three phase leg are either connected to positive rail or negative rail so they have no impact on DC neutral point. Zero vectors short circuits the load to either positive rail, negative rail or midpoint of the capacitors [13]. The neutral point potential is also independent of this group of vector. In medium vector, one of the three phase is connected to neutral point and the remaining two phase legs are connected to +ve and −ve rail respectively. So in this case the neutral point potential deviates from zero. In small vector group, one or two phase is always connected to the DC midpoint while the remaining phase leg is connected to either +ve rail or −ve rail. The direction of neutral current depends on the nature of load current. Either the load current will inject into or extract from the neutral point. It also has an impact on the variation of DC potential. The small vector is further classified into positive small vector or negative small vector. The positive small vector is obtained when load current charges the upper capacitor and discharges the lower capacitor. The vice versa is responsible for the creation of negative small vector. These two vectors are drawn in fig.18.
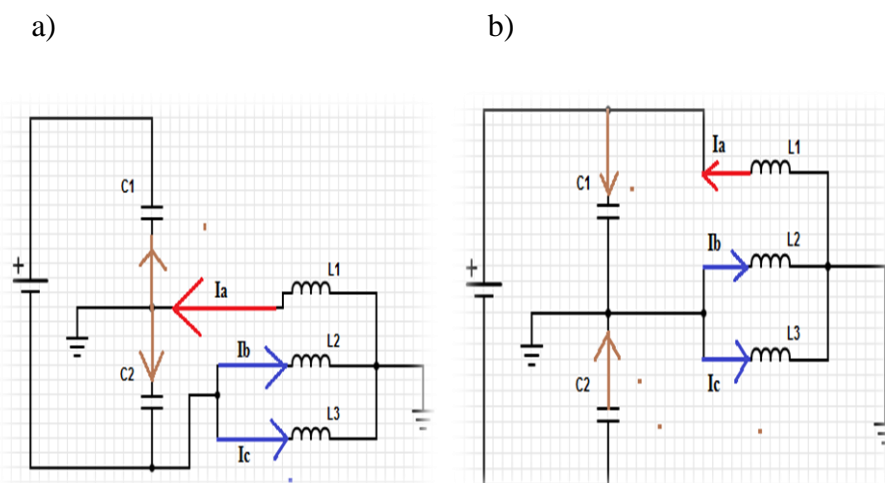
a)   b)

Figure 18 Small vector effects on DC neutral point a) negative small vector (0--)

b) positive small vector (+00)

From the basic circuit theory,

$$i_o = i_{C_1} - i_{C_2}$$ (25)

where,

$$i_{C_1} = C_1 \frac{du_{C_1}}{dt} \quad \text{and} \quad i_{C_2} = C_2 \frac{du_{C_2}}{dt}$$

$$u_{C_1} = \frac{u_{DC}}{2} - u_o \ \text{and} \ u_{C_2} = u_o - \left(\frac{-u_{DC}}{2} \right)$$

The two capacitors should be match to each other gives,

$$C_1 = C_2 = C$$

$$i_o = c \frac{d\left(\frac{u_{DC}}{2} - u_o \right)}{dt} - c \frac{d\left(u_o + \frac{u_{DC}}{2} \right)}{dt}$$

$$i_o = c \frac{d\left(\frac{u_{DC}}{2} - u_o - u_o - \frac{u_{DC}}{2} \right)}{dt} \quad \rightarrow \quad i_o = c \frac{d\left(-2u_o \right)}{dt}$$

$$\frac{du_o}{dt} = -\frac{i_o}{2C}$$ (26)

Form the above equation it is deduce that the neutral current (i_o) is dependent on neutral point potential (u_o).

The small vector has a redundant vector while remaining vector doesn't. These two redundant vectors have same amplitude but the direction of current flow is opposite causing a cancelling effect at the neutral point makes the neutral point potential stable. These two redundant vectors are used to control the neutral point potential. The duty cycle of positive and negative small vectors are combined together to get the total duty cycle of small vector [21].

$$d_s = d_{s,p} + d_{s,n}$$

Where,

d_s = duty cycle of small vector

$d_{s,p}$ = duty cycle of positive small vector

$d_{s,n}$= duty cycle of negative small vector

By proper adjusting the duty cycle of these two redundant vectors the neutral point will be stable. Table 5 shows the state of neutral current when medium and small vectors are applied.

Table 5 Status of neutral current

Small Vector	Neutral current	Small Vector	Neutral current	Medium Vector	Neutral current
+00	$-i_a$	-00	$-i_a$	+0-	i_b
0--	i_a	0++	i_a	0+-	i_a
00-	$-i_c$	--0	i_c	-+0	i_c
++0	i_c	00+	$-i_c$	-0+	i_b
-0-	i_b	+0+	i_b	0-+	i_a
0+0	$-i_b$	0-0	$-i_b$	+-0	i_c

Consider the region I of sector I for one complete cycle, V_4 (0--) and V_8(00-) must be switched during half cycle and for the next half cycle the V_3(+00) and V_7(++0). V_4injectsi_a current and V_3 extract $-i_a$ current. Similarly V_7 injects i_c current and V_8 extract $-i_c$ current.

$$i_{NP1} = d_4 V_4 + d_8 V_8 \rightarrow i_{NP1} = d_4(i_a) + d_8(-i_c)$$

$$i_{NP2} = d_3 V_3 + d_7 V_7 \rightarrow i_{NP2} = d_3(-i_a) + d_7(i_c)$$

$$i_{o=}i_{NP1} + i_{NP2} = 0$$

where d$_3$, d$_4$, d$_7$ and d$_8$ are the duty cycles of the corresponding vector.

While keep this into mind, the available switching schemes are discussed in next section.

3.6.1 Implementation of different switching scheme

This section describes the need of different switching schemes i.e. 7-segment switching scheme, 9-segment switching scheme and 13-segment switching scheme which

incorporates the switching of one phase at a time to mitigate the problem of harmonics. The waveform of these switching segments will be drawn in support of this statement.

Table 6 Switching pattern of sector I

Region	Switching Vectors												
	13-segments switching pattern												
	1	2	3	4	5	6	7	8	9	10	11	12	13
I	V_2	V_4	V_8	V_1	V_3	V_7	V_{27}	V_7	V_3	V_1	V_8	V_4	V_2
	---	0--	00-	000	+00	++0	+++	++0	+00	000	00-	0--	---

Region	7-segment switching pattern						
II	1	2	3	4	5	6	7
	V_4	V_5	V_6	V_3	V_6	V_5	V_4
	0--	+--	+0-	+00	+0-	+--	0--

Region	9-segment switching pattern								
III	1	2	3	4	5	6	7	8	9
	V_4	V_8	V_6	V_3	V_7	V_3	V_6	V_8	V_4
	0--	00-	+0-	+00	++0	+00	+0-	00-	0--

Region	7-segments switching pattern						
IV	1	2	3	4	5	6	7
	V_8	V_6	V_9	V_7	V_6	V_9	V_8
	00-	+0-	++-	++0	++-	+0-	00-

From table 6, it is concluded that only one phase is switched during each transition. For e.g. in region II the transition from sequence 1 to sequence 2, R-φ is switched from 0 → + while the Y-φ and B-φ remains on their previous value i.e. '-'.
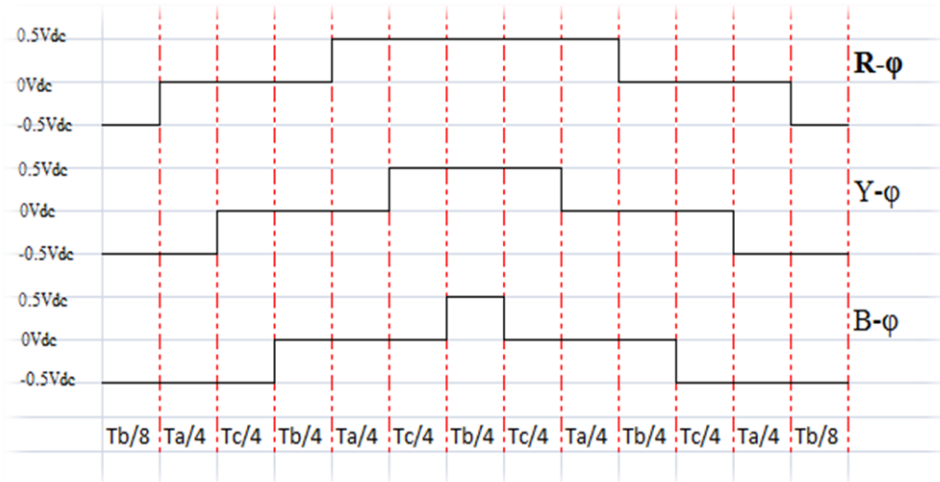
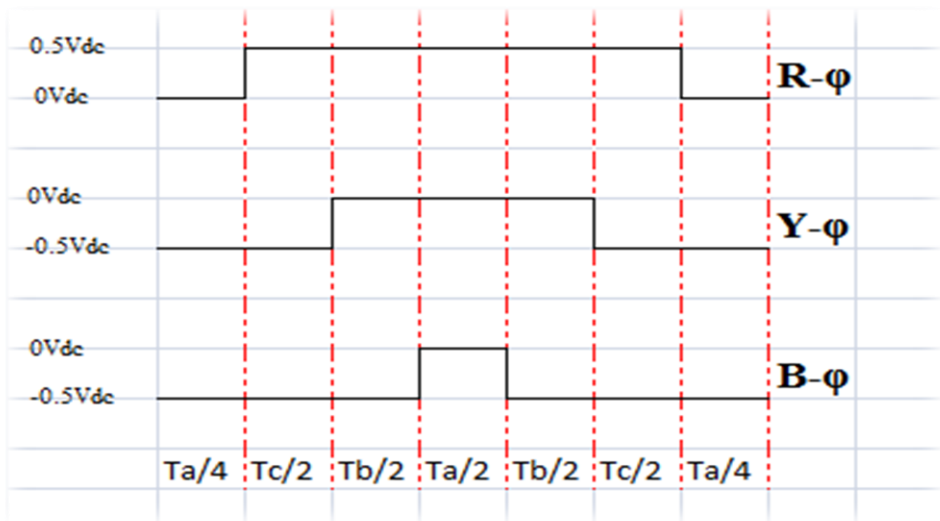*Figure 19 13-segment switching pattern for sector I, region I*

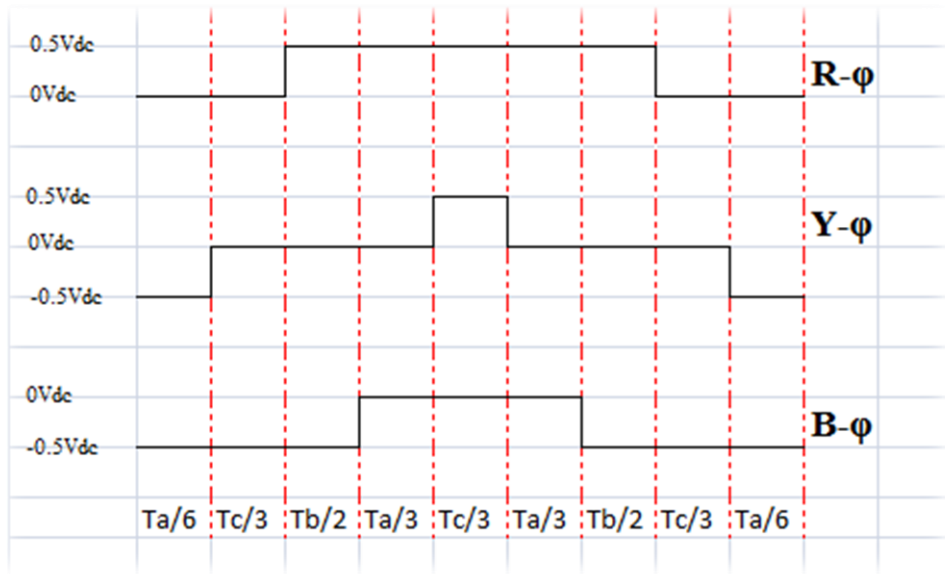*Figure 20 7-segment switching pattern for sector I, region II*

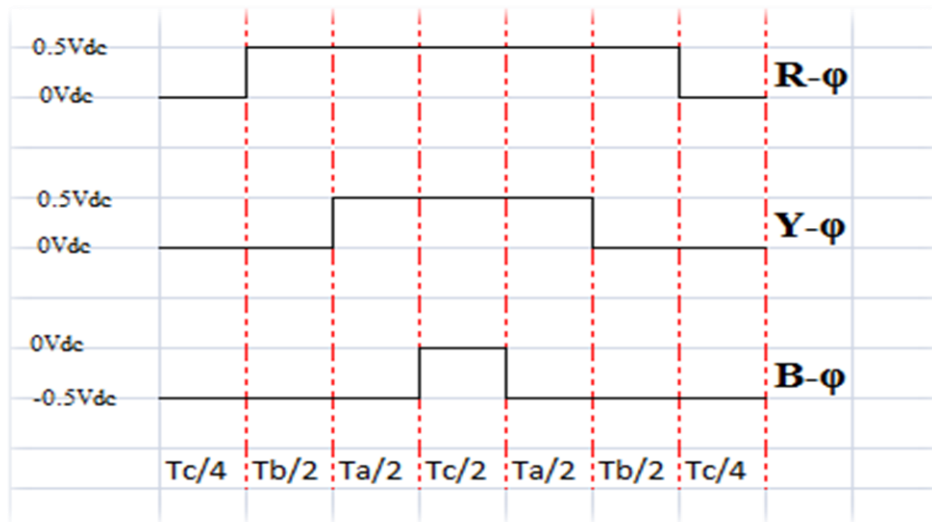*Figure 21 9-segment switching pattern for sector I, region III*

Figure 22 7-segments switching for sector I, region IV

Switching schemes for the remaining sectors are given in Appendix-IX.

3.7 Duty Cycle Calculation

In this section the duty cycle of 3-phases will be calculated for all 4 region of sector I which means for how much time all these 3-phases will remain ON from the entire Ts second. From the above figures there are only three different DC levels available i.e. $\frac{1}{2}Vdc$, 0Vdc, $-\frac{1}{2}Vdc$, the ratio of the sum of the product of these levels with their corresponding time duration to the total sampling time (Ts) gives the duty ratio.

13-segment switching scheme (Sector I and Region I):

For the R-φ

$$R=\frac{1}{2}Vdc\left[\frac{Ta}{4}+\frac{Tc}{4}+\frac{Tb}{4}+\frac{Tc}{4}+\frac{Ta}{4}\right]-\frac{1}{2}Vdc\left[\frac{Tb}{8}+\frac{Tb}{8}\right]$$

$$R=\frac{1}{2}Vdc\left[\frac{2Ta+2Tc+2Tb+2Tc+2Ta-Tb-Tb}{8}\right]\rightarrow\frac{1}{2}Vdc\left[\frac{1}{2}Ta+\frac{1}{2}Tc\right]$$

$$D_R=\frac{\left[\frac{1}{2}Ta+\frac{1}{2}Tc\right]}{Ts}$$

For the Y-φ

$$Y=\frac{1}{2}Vdc\left[\frac{Tc}{4}+\frac{Tb}{4}+\frac{Tc}{4}\right]-\frac{1}{2}Vdc\left[\frac{Tb}{8}+\frac{Ta}{4}+\frac{Ta}{4}+\frac{Tb}{8}\right]$$

$$Y=\frac{1}{2}Vdc\left[\frac{2Tc+2Tb+2Tc-Tb-2Ta-2Ta-Tb}{8}\right]$$

$$D_Y=\frac{\left[-\frac{1}{2}Ta+\frac{1}{2}Tc\right]}{Ts}$$

For the B-φ

$$B=\frac{1}{2}Vdc\left[\frac{Tb}{4}\right]-\frac{1}{2}Vdc\left[\frac{Tb}{8}+\frac{Ta}{4}+\frac{Tc}{4}+\frac{Tc}{4}+\frac{Ta}{4}+\frac{Tb}{8}\right]$$

$$B=\frac{1}{2}Vdc\left[\frac{2Tb-Tb-2Ta-2Tc-2Tc-2Ta-Tb}{8}\right]$$

$$D_B=\frac{\left[-\frac{1}{2}Ta-\frac{1}{2}Tc\right]}{Ts}$$

7-segment switching scheme (Sector I and region II):

For R- φ

$$R=\frac{1}{2}Vdc\left[\frac{Tc}{2}+\frac{Tb}{2}+\frac{Ta}{2}+\frac{Tb}{2}+\frac{Tc}{2}\right]$$

$$R=\frac{1}{2}Vdc\left[\frac{Ta+2Tb+2Tc}{2}\right]\rightarrow\frac{1}{2}Vdc\left[\frac{1}{2}Ta+Tb+Tc\right]$$

$$D_R=\frac{\left[\frac{1}{2}Ta+Tb+Tc\right]}{Ts}$$

For Y- φ

$$Y = -\frac{1}{2}Vdc\left[\frac{Ta}{4} + \frac{Tc}{2} + \frac{Tc}{2} + \frac{Ta}{4}\right]$$

$$Y = -\frac{1}{2}Vdc\left[\frac{Ta+2Tc+2Tc+Ta}{4}\right] \rightarrow \frac{1}{2}Vdc\left[\frac{Ta}{2} + Tc\right]$$

$$D_Y = \frac{\left[\frac{1}{2}Ta+Tc\right]}{Ts}$$

For the B-φ

$$B = -\frac{1}{2}Vdc\left[\frac{Ta}{4} + \frac{Tc}{2} + \frac{Tb}{2} + \frac{Tb}{2} + \frac{Tc}{2} + \frac{Ta}{4}\right]$$

$$B = -\frac{1}{2}Vdc\left[\frac{Ta+2Tc+2Tb+2Tb+2Tc+Ta}{4}\right] \rightarrow -\frac{1}{2}Vdc\left[\frac{2Ta+4Tb+4Tc}{4}\right]$$

$$D_B = \frac{\left[\frac{1}{2}Ta+Tb+Tc\right]}{Ts}$$

9-segment switching scheme (Sector I and region III)

For R- φ

$$R = \frac{1}{2}Vdc\left[\frac{Tb}{2} + \frac{Ta}{3} + \frac{Tc}{3} + \frac{Ta}{3} + \frac{Tb}{2}\right]$$

$$R = \frac{1}{2}Vdc\left[\frac{3Tb+2Ta+2Tc+2Ta+3Tb}{6}\right] \rightarrow \frac{1}{2}Vdc\left[\frac{2}{3}Ta + Tb + \frac{1}{3}Tc\right]$$

$$D_R = \frac{\left[\frac{2}{3}Ta+Tb+\frac{1}{3}Tc\right]}{Ts}$$

For the Y-φ

$$Y = \frac{1}{2}Vdc\left[\frac{Tc}{3}\right] - \frac{1}{2}Vdc\left[\frac{Ta}{6} + \frac{Ta}{6}\right]$$

$$Y = \frac{1}{2}Vdc\left[\frac{2Tc-Ta-Ta}{6}\right]$$

$$D_Y = \frac{\left[-\frac{1}{3}Ta+\frac{1}{3}Tc\right]}{Ts}$$

For the B-φ

$$B = -\frac{1}{2}Vdc\left[\frac{Ta}{6} + \frac{Tc}{3} + \frac{Tb}{2} + \frac{Tb}{2} + \frac{Tc}{3} + \frac{Ta}{6}\right]$$

$$B = -\frac{1}{2}Vdc\left[\frac{2Ta+4Tc+6Tb}{6}\right]$$

$$D_B = \frac{\left[\frac{1}{3}Ta + Tb + \frac{2}{3}Tc\right]}{Ts}$$

7-segment switching scheme (Sector I and region IV)

For R- φ

$$R = \frac{1}{2}Vdc\left[\frac{Tb}{2} + \frac{Ta}{2} + \frac{Tc}{2} + \frac{Ta}{2} + \frac{Tb}{2}\right]$$

$$R = \frac{1}{2}Vdc\left[\frac{2Ta + 2Tb + Tc}{2}\right] \rightarrow \frac{1}{2}Vdc\left[Ta + Tb + \frac{Tc}{2}\right]$$

$$D_R = \frac{\left[Ta + Tb + \frac{1}{2}Tc\right]}{Ts}$$

For Y- φ

$$Y = \frac{1}{2}Vdc\left[\frac{Ta}{2} + \frac{Tc}{2} + \frac{Ta}{2}\right]$$

$$Y = \frac{1}{2}Vdc\left[\frac{2Ta + Tc}{2}\right] \rightarrow \frac{1}{2}Vdc\left[\frac{Tc}{2} + Ta\right]$$

$$D_Y = \frac{\left[\frac{1}{2}Tc + Ta\right]}{Ts}$$

For the B-φ

$$B = -\frac{1}{2}Vdc\left[\frac{Tc}{4} + \frac{Tb}{2} + \frac{Ta}{2} + \frac{Ta}{2} + \frac{Tb}{2} + \frac{Tc}{4}\right]$$

$$B = -\frac{1}{2}Vdc\left[\frac{4Ta + 4Tb + 2Tc}{4}\right]$$

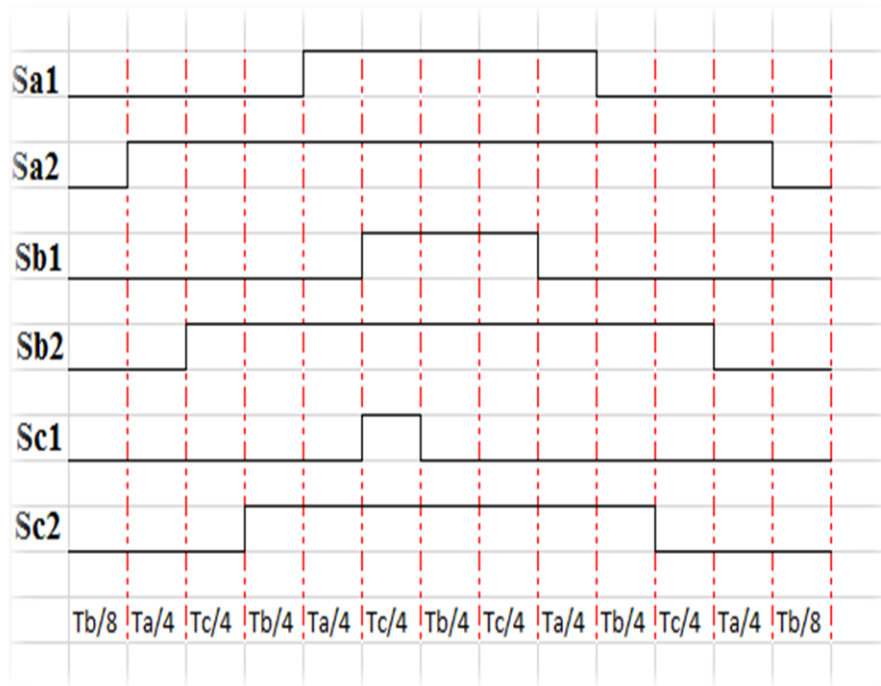$$D_B = \frac{\left[Ta + Tb + \frac{1}{2}Tc\right]}{Ts}$$

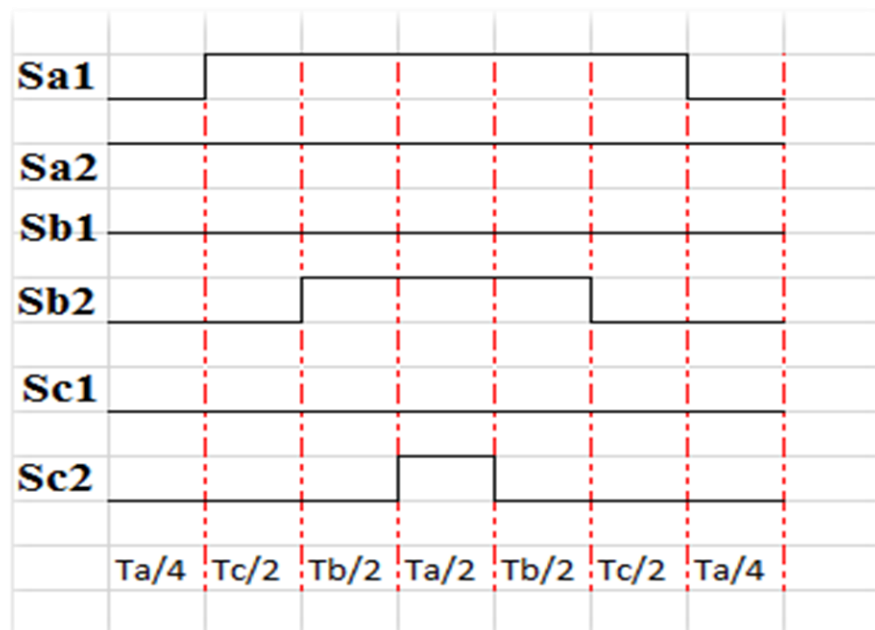*Figure 23 a) Gating signal pattern of sector I, region I [18]*

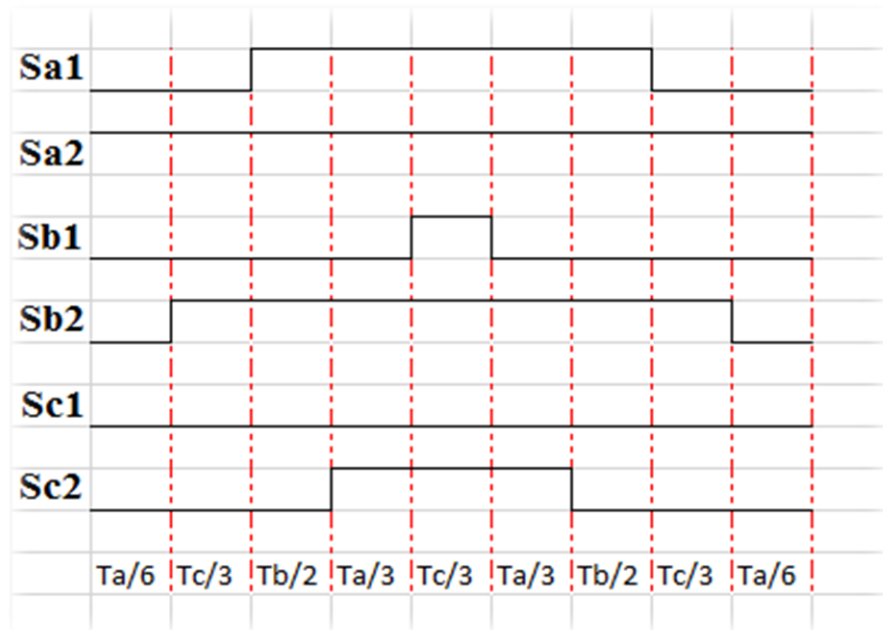*Figure 23 b) Gating signal pattern of sector I, region II [18]*

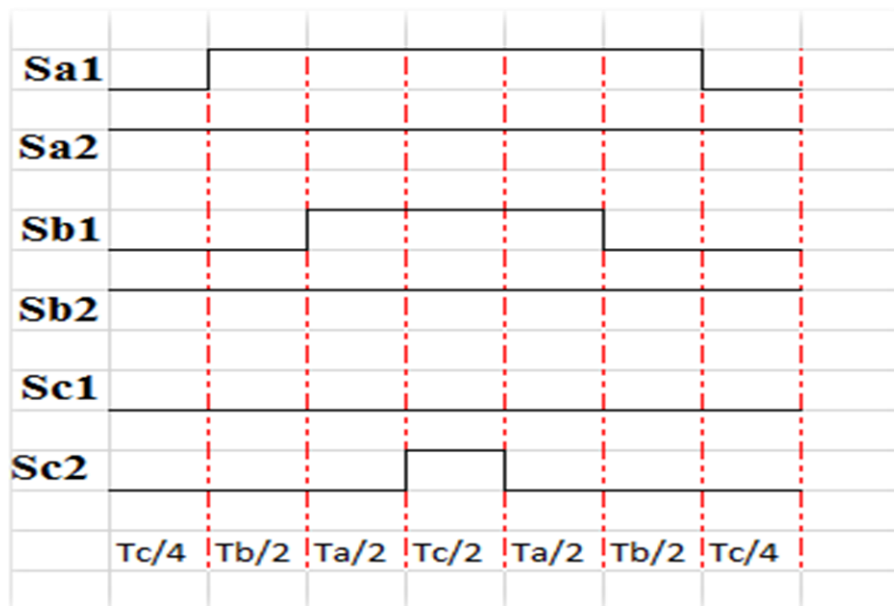*Figure 23 c) Gating signal pattern of sector I, region III [18]*

Figure 23 d) Gating signal pattern of sector I, region IV [18]

3.8 DC Link Current

In order to write the equation of DC side current, the three pole voltages i.e. V_{Ro}, V_{Yo} and V_{Bo} must be written in terms of their switching functions. The switching function can be either,

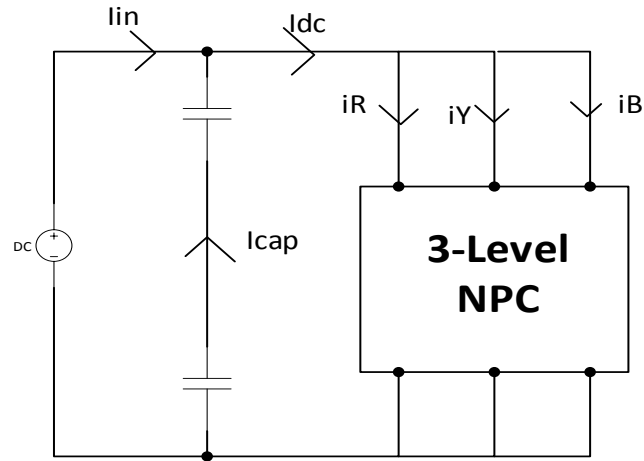$S_x = 1$(ON) or 0(OFF), x= phase leg

Figure 24 DC link current and each phase leg current

$$V_{RO=}(S_R - 0.5)V_{DC} \qquad V_{YO=}(S_Y - 0.5)V_{DC} \qquad V_{BO=}(S_B - 0.5)V_{DC}$$

For 3-φ star connected balanced load,

$$V_{RN} = \frac{V_{RY} - V_{BR}}{3} \qquad V_{YN} = \frac{V_{YB} - V_{RY}}{3} \qquad V_{BN} = \frac{V_{BR} - V_{YB}}{3}$$

For RL load,

$$V_{RN} = Ri_R + L\frac{di_R}{dt} \qquad \rightarrow \qquad \frac{di_R}{dt} = \frac{V_{RN} - Ri_R}{L}$$

After integrating on both sides gives the R-phase current,

$$i_R = \int_0^{2\pi} \frac{V_{RN} - Ri_R}{L}$$

Similarly for Y-φ,

$$V_{YN} = Ri_Y + L\frac{di_Y}{dt} \qquad \rightarrow \qquad \frac{di_Y}{dt} = \frac{V_{YN} - Ri_Y}{L}$$

After integrating on both sides gives the Y-phase current,

$$i_Y = \int_0^{2\pi} \frac{V_{YN} - Ri_Y}{L}$$

For B-φ,

$$V_{BN} = Ri_B + L\frac{di_B}{dt} \qquad \rightarrow \qquad \frac{di_B}{dt} = \frac{V_{BN} - Ri_B}{L}$$

After integrating on both sides gives the B-phase current,

$$i_B = \int_0^{2\pi} \frac{V_{BN} - Ri_B}{L}$$

In general the DC link current is represented as,

$$i_{DC} = S_R i_R + S_Y i_Y + S_B i_B$$

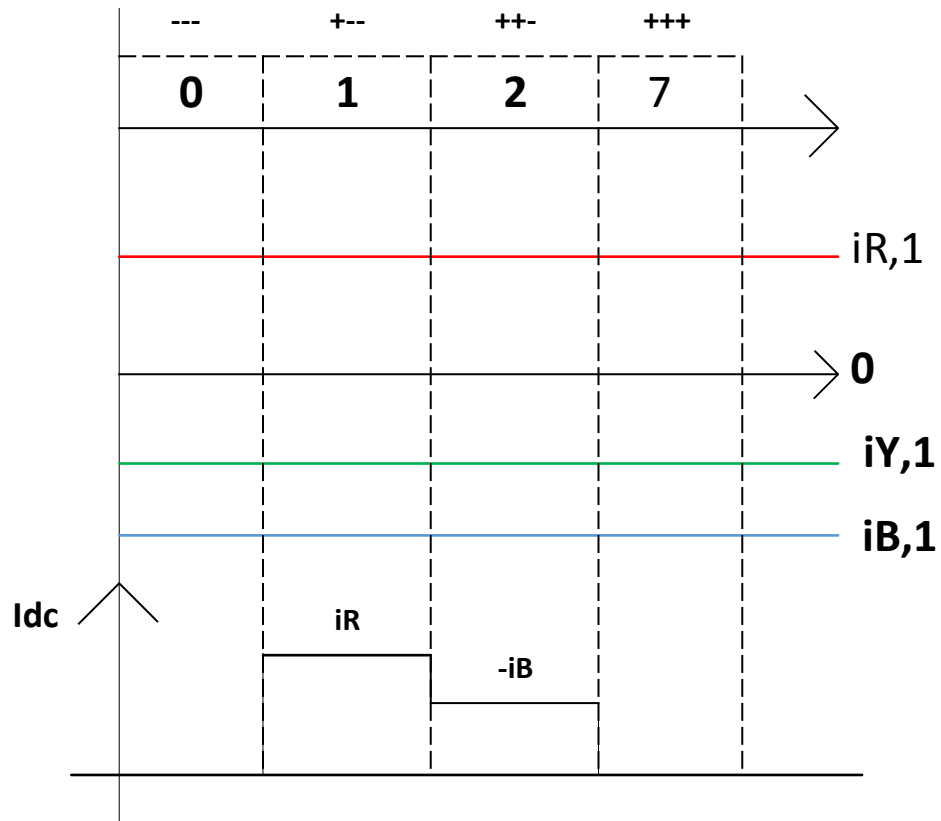### 3.8.1 Average DC Link Current over a Sub-cycle:

Figure 25 DC link current over a sub-cycle

$$\frac{1}{T_s}\int_0^{T_s} i_{DC}\partial t = \frac{1}{T_s}\int_0^{T_s} \left(S_R i_R + S_Y i_Y + S_B i_B\right)\partial t$$

The left hand side of the above equation represents the average DC link current.

$$i_{DC,avg} = \frac{1}{T_s} i_{R,1} \int_0^{T_s} S_{R,1} + \frac{1}{T_s} i_{Y,1} \int_0^{T_s} S_{Y,1} + \frac{1}{T_s} i_{B,1} \int_0^{T_s} S_{B,1}$$

Where $i_{R,1}$= Fundamental component of R-phase current

$\quad\quad$ $I_{Y,1}$= Fundamental component of Y-phase current

$\quad\quad$ $I_{B,1}$= Fundamental component of B-phase current

The terms except $i_{R,1}$, $i_{Y,1}$, $i_{B,1}$ on the right hand side of the above equation forms a duty ratio of each phase leg.

$$i_{DC,avg} = D_R i_{R,1} + D_Y i_{Y,1} + D_B i_{B,1}$$

The duty ratio of R-φ, Y-φ and B-φ can be written as,

$$D_R = \frac{T_{ON,R+}}{T_s} \quad\quad\quad\quad D_Y = \frac{T_{ON,Y+}}{T_s} \quad\quad\quad\quad D_B = \frac{T_{ON,B+}}{T_s}$$

The input DC current (I_{in}) is the average of DC link current (I_{DC}) over a cycle.

$$I_{in} = \frac{1}{2\pi} \int_0^{2\pi} i_{DC,avg} \partial(\omega t)$$

3.9　Conclusion

In this chapter the theory, concept and background of three-level SVPWM has been discussed in detail. In support of this statement power stage of NPC has been developed. To develop space vector diagram mathematical calculation has been done along with the different switching schemes to reduce total harmonic distortion. The derivation of pole voltages with supporting waveform has been done based on the selection of particular sector and region. Vector switching times is also calculated along with the duty ratio of power switches.
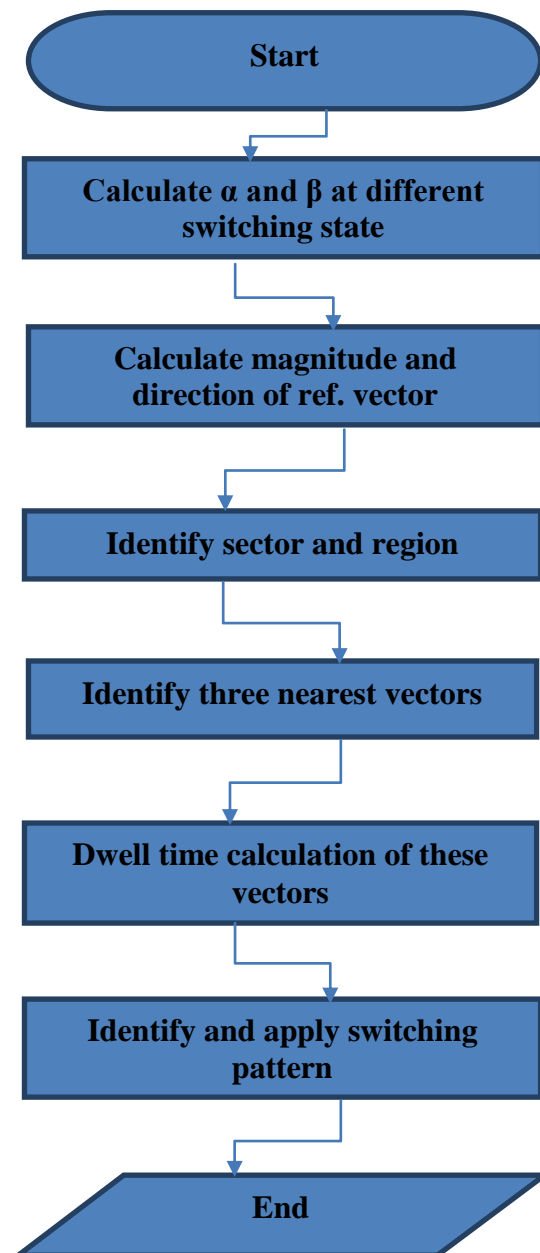
3.10 FLOW CHART OF THE ALGORITHM

Figure 26 SVPWM algorithm representations in flow chart

4. SIMULATIONS & RESULTS

4.1 Introduction

A simulation is a tool through which any physical process can be implemented to get the behavior of that system. From the results obtained from simulations are very much same as in physical environment. As far as this thesis is concerned, the simulation tool box used for the implementation of three-level SVPWM algorithm is MATLAB/Simulink. MATLAB environment provides the built-in library features. The Simulink model contains different blocks to implement this algorithm included some sub blocks and MATLAB Function blocks where the C-language code is generated. The power circuit for three level SVPWM is generated with 12-IGBT's and producing an inverter output with fundamental frequency of 50 Hz by incorporated 3-φ star connected balance load.

The "Subsystem block" employs the Clark's transformation to convert three phase quantities to stationary reference frame which is based on eq. 2.15 and 2.16. The "Subsystem1 block" is the representation of sector selection which is fed from the results obtained from Clark's transformation. The "Matlab Function1 block" employs the criteria for region selection based on the values of X_1, X_2 and X_n discuss in section 3.4.5. The "Matlab Function block" performs a very important task, the dwell time (Ta, Tb and Tc) calculation and vector switching states are performed simultaneously. This block cannot run until or unless the earlier three blocks produce its output. In other words, the outputs of these three blocks are cascaded to "Matlab Function block". The gating signals are generated as an output from this block which further drives the power stage of NPC inverter. The scopes are connected in such a way that the line to neutral and line to line voltage waveform are drawn.

4.2 Output from Clark's transformation

The magnitude and angle of reference vector is shown in fig.27 and 28. The sub-blocks of the main block is present in Appendix-I.
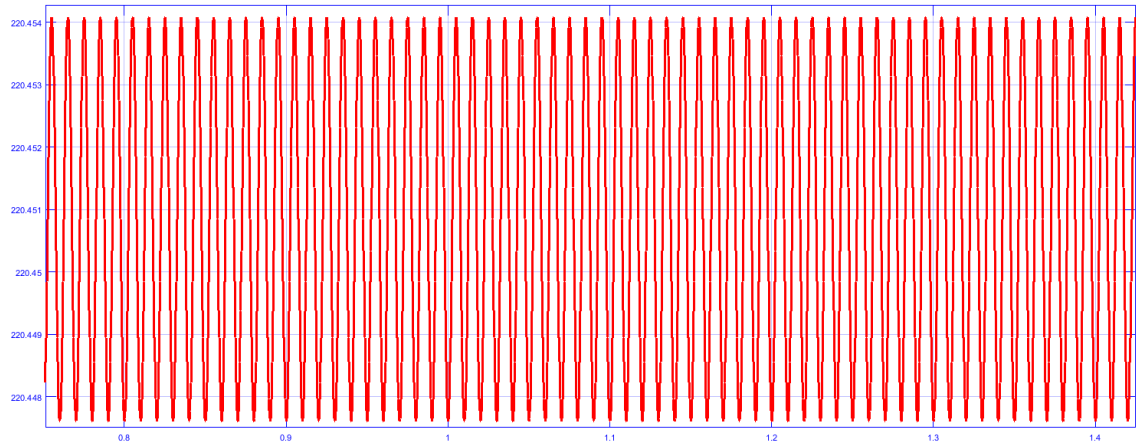
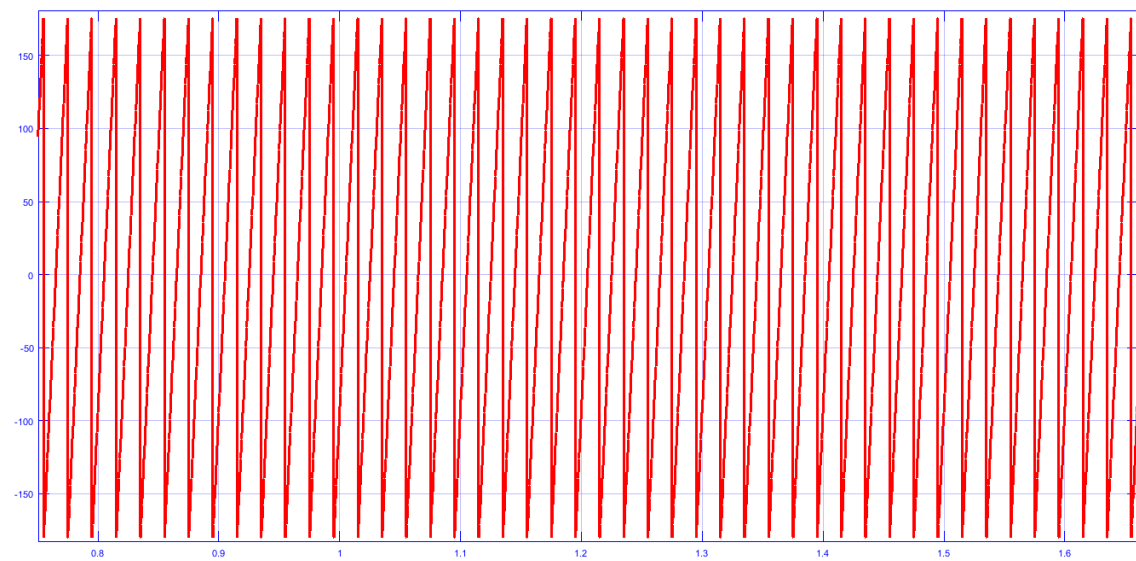*Figure 27 Magnitude of reference vector*

Figure 28 Angular position of reference vector

4.3   Sector Selector

The sector selection block is driven with an angle. Some mathematical function and logical functions have been incorporated to identify the sector. From the fig.29 the reference vector passes through each sector with a fix step.
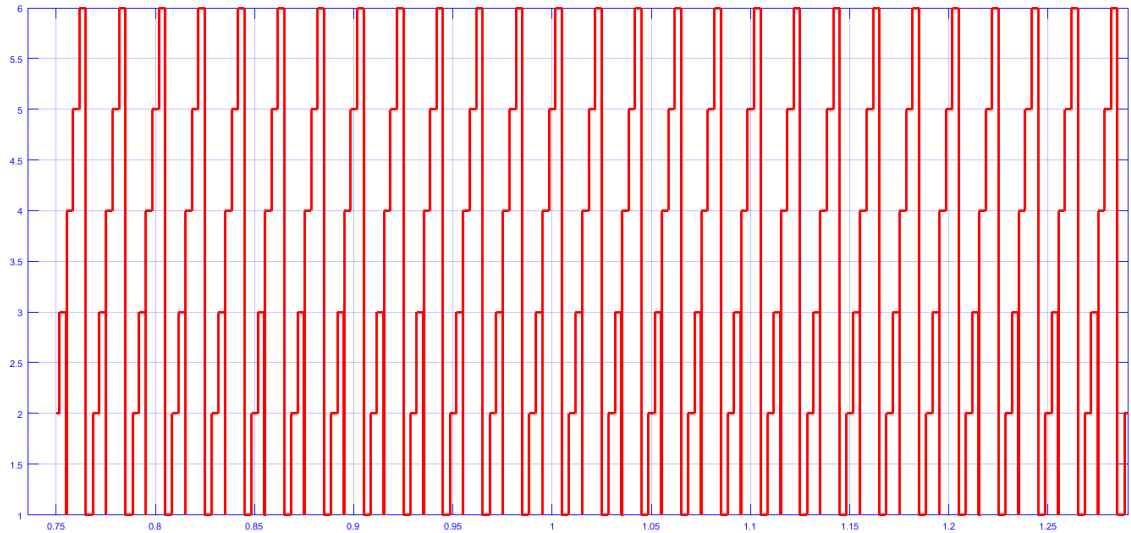
Figure 29 Output of sector determination block

The brief description of "Sector selection" block is given in Appendix-II

4.4 Region Selector

The entire space vector diagram is divided into 6-sectors, each sector has a same methodolgy for switching stationary vectors. After each 60° degrees the new sector arrived and same strategy is applied over it which makes the system more complex. The alternate way is to bring back each sector to sector I or in other words each sector is multiple of 60°. The resulting angle is obtained by subtracting the calculated angle from multiple of 60 as given below,

Alpha=angle–(sector-1)60   (27)

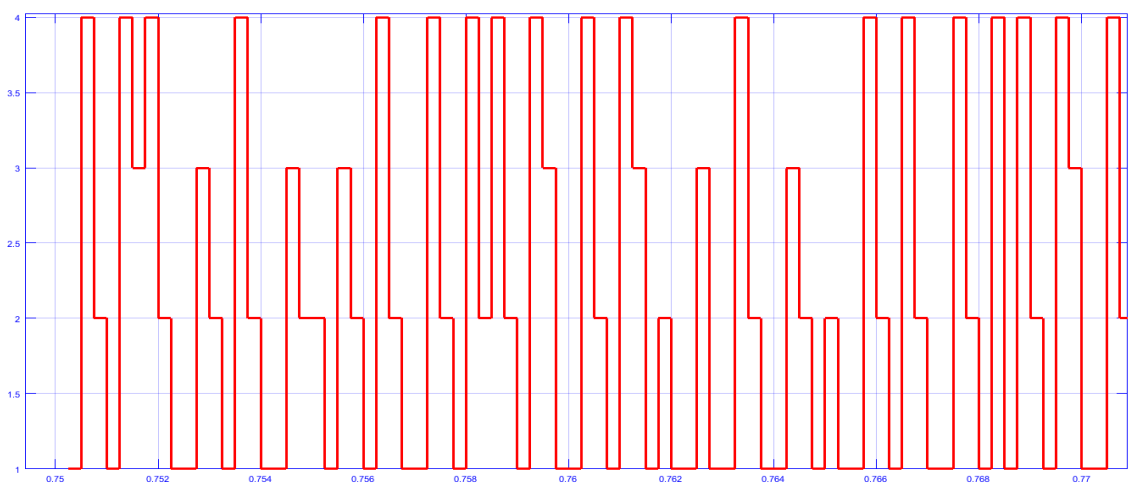The contents of region selection is given in Appendix-III.

Figure 30 Output of region selection block

The "dwell time calculations" block performs the calculation for the dwell time of each region of sector I (Ta_x, Tb_x, Tc_x) where x= region number. The input necessary to drive this block requires sector number, region number, modulation index, magnitude and angle of reference vector. The outputs are 12 dwell time signals. The sub-block is the implementation of equations given in table 4. Based on these values the stationary vectors are applied for that much of duration. The contents of this block are presented in Appendix-IV.

4.5   Gating Signal Generator

The output of this block also generates the gating signals to drive the power switches in NPC. The bottom two switches of each phase leg are connected in complementary fashion so for these switches gating signals are generated by inverted the status of upper two switches.
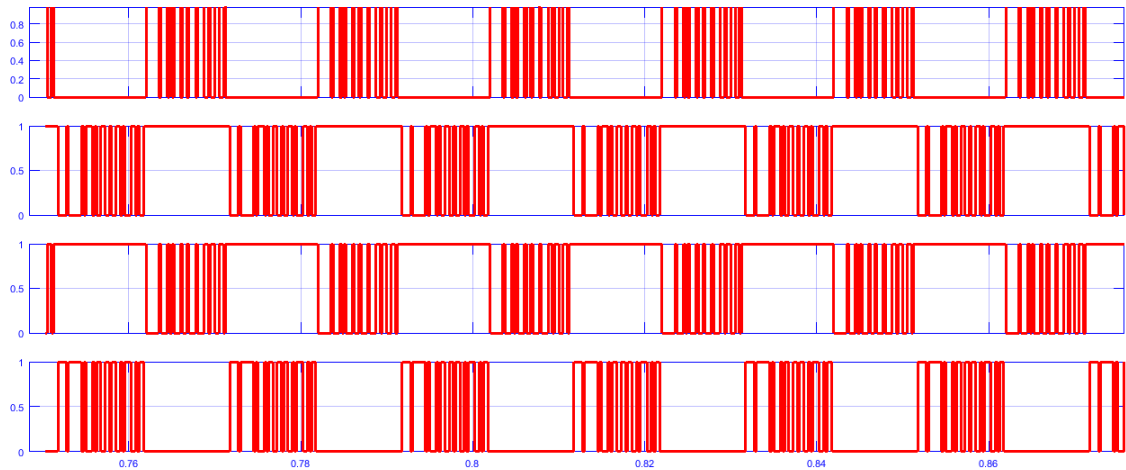

Figure 31 Gating signal for R-phase leg (i) SA1 (ii) SA1' (iii) SA2 (iv) SA2'

After the implementation of theory described in the above section gives the pole voltage which is measured from the middle of each phase leg to the DC neutral point 'o'. The NPC inverter is operated with 440V DC input which produces an output having a three level i.e. 220V, 0V and -220V.

The **SimPowerSystem** is a modern design tool used to employ the NPC inverter. It uses Simulink in order to implement its features. Not only can draw electrical circuit and power network rapidly [7] but analyze the data in an efficient manner.

4.6   Model Parameters

These simulation runs with the following parameters,

Vdc= 440V, m= 0.95, fs= 2 kHz, R_{load}= 10Ω, L_{load}= 15mH and f_1= 50Hz.

IGBT is selected as a power switch for three-level NPC inverter having following features,

Internal resistance = R_{ON}= 1mΩ

Snubber Resistance=R_s=1e5Ω

Snubber Capacitance =C_S= Inf

4.7 Line-to-Neutral Voltage with Harmonic Analysis
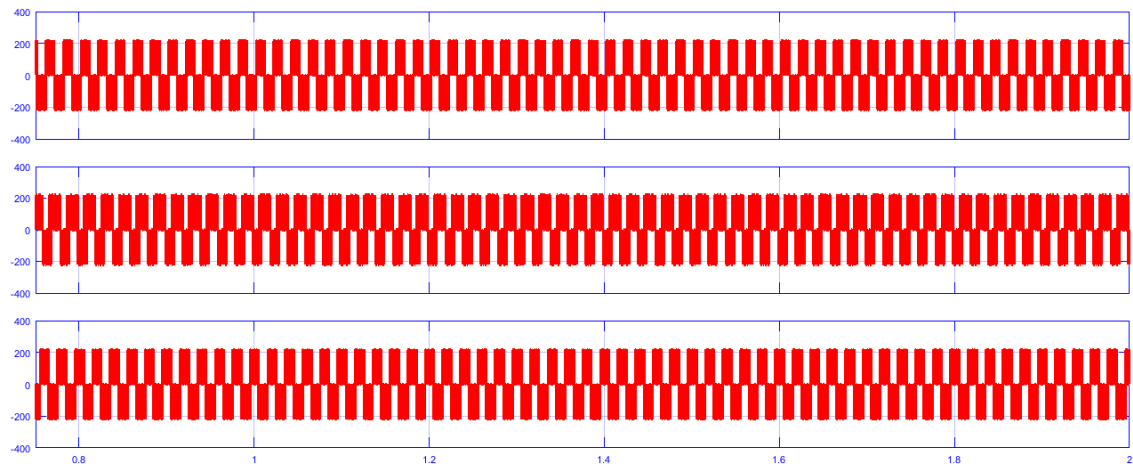
Figure 32 3-phase line-to-neutral voltages

These are the three phase pole voltages or line-to-neutral voltages before passing through the filter so it contain harmonics contents which must be removed before the load. In order to investigate about the harmonics, SimPowerSystems equipped with special feature known as power gui block which contain FFT analysis. The harmonic analysis for the remaining phases is given in Appendix- V and VI respectively.
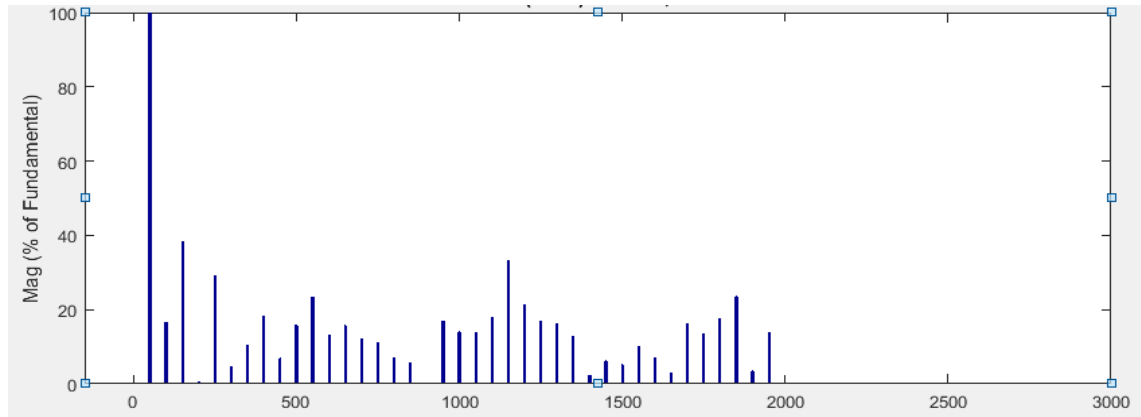
a)
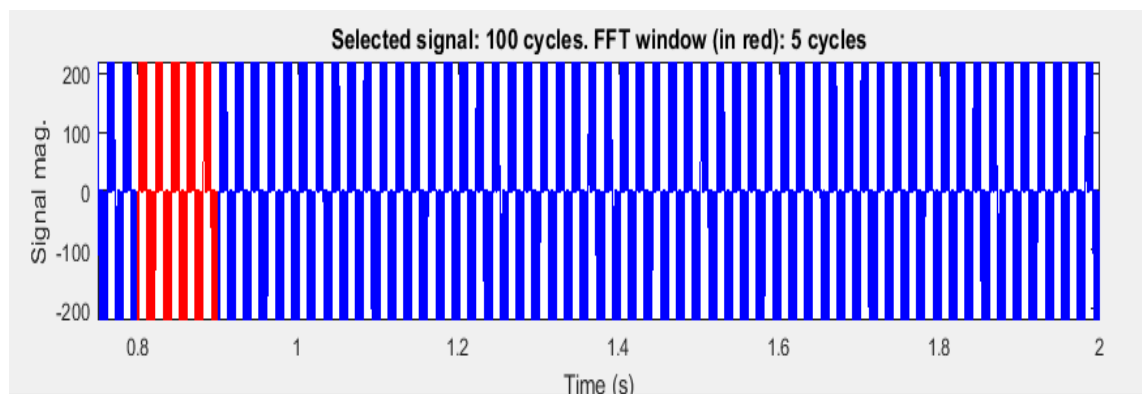
b)

Figure 33 Analysis of R-φ voltage a) FFT window of R-phase leg b) Harmonic profile of R-phase leg

4.8   Line-to-Line Voltage with Harmonic Analysis

The line to line voltage is obtained as the potential difference between two lines with DC neutral point 'o' as the reference. But we are interested in load neutral point 'n' rather than 'o'. So for convenience the phase voltages and line to line voltages are regarded as,

Phase voltages: V_{ro}, V_{yo}, V_{bo}.

Line to Line voltages: $V_{ry}= V_{ro}-V_{yo}$, $V_{yb}=V_{yo}-V_{bo}$, $V_{br}= V_{bo}-V_{ro}$

For 3-φ star connected balance load, the relationship between DC neutral point 'o' and load neutral point 'n' is given by,

$$V_{no}= \frac{V_{ro} +V_{yo} +V_{bo}}{3}$$

$$V_{rn}= V_{ro}-V_{no}$$

$$V_{rn}= V_{ro}- \frac{V_{ro} +V_{yo} +V_{bo}}{3} \rightarrow V_{rn}=\frac{2V_{ro} -V_{yo} -V_{bo}}{3}$$

Each pole voltage can have only 3 possible values either $0V_{dc}$, $+\frac{V_{dc}}{2}$, $-\frac{V_{dc}}{2}$. On the basis these value 5 combinations are possible for line to line voltages either $+V_{dc}$, $-V_{dc}$, $0V_{dc}$, $+\frac{V_{dc}}{2}$, $-\frac{V_{dc}}{2}$.
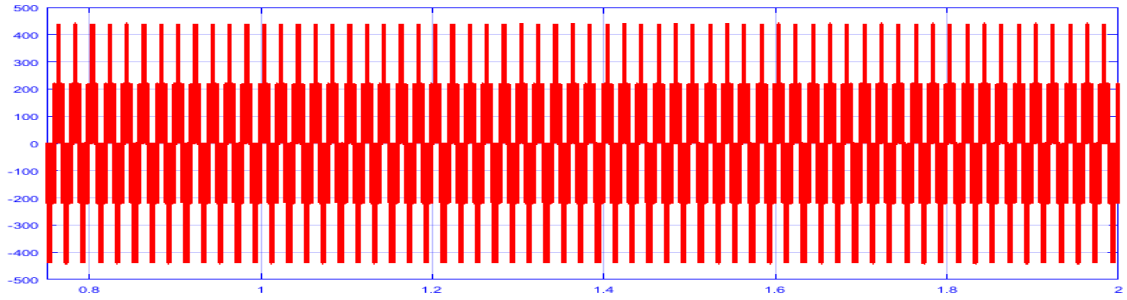
Figure 34 Line-to-Line voltages between R-phase and Y-phase

a)
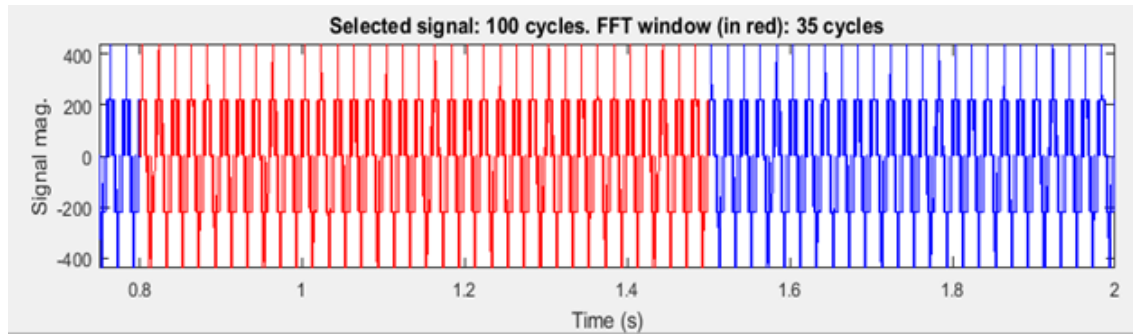
b)
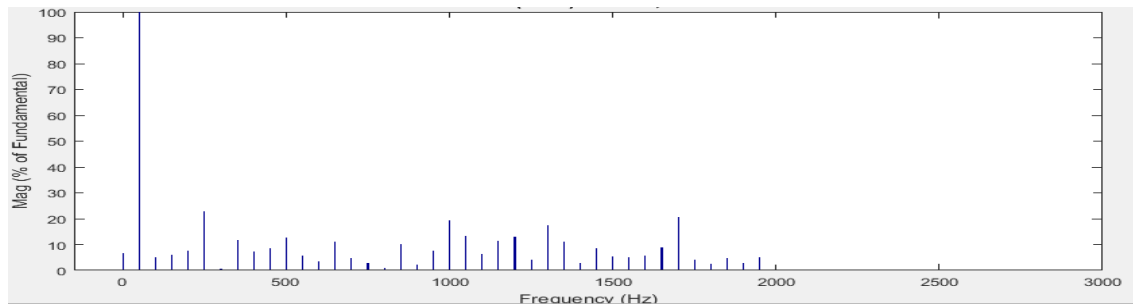
Figure 35 Analysis of line- to-line voltage a) FFT window of line-to-line voltage

b) Harmonic profile of line-to-line voltage

4.9 Implementation of Filter

The output produce by an inverter contain some harmonic contents which need to be removed before applying it to the load. Only the fundamental component is allowed to pass to the load. These harmonic can be separated from its harmonic contents by designing a filter having a resonant frequency of 50Hz.

$$f_r = \frac{1}{2\pi\sqrt{LC}} \rightarrow LC = 1.012949 * 10^{-5}$$

By deduce the above value gives, L=6.330mH and C=1600μF.

a)
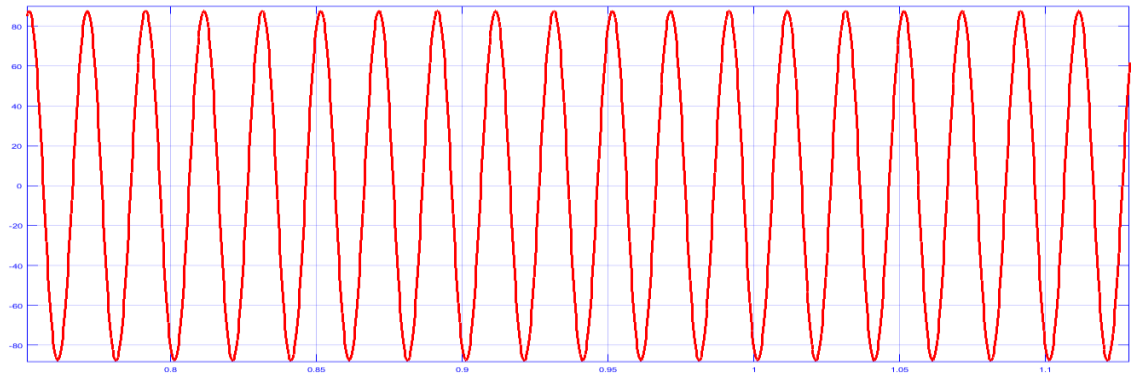
b)
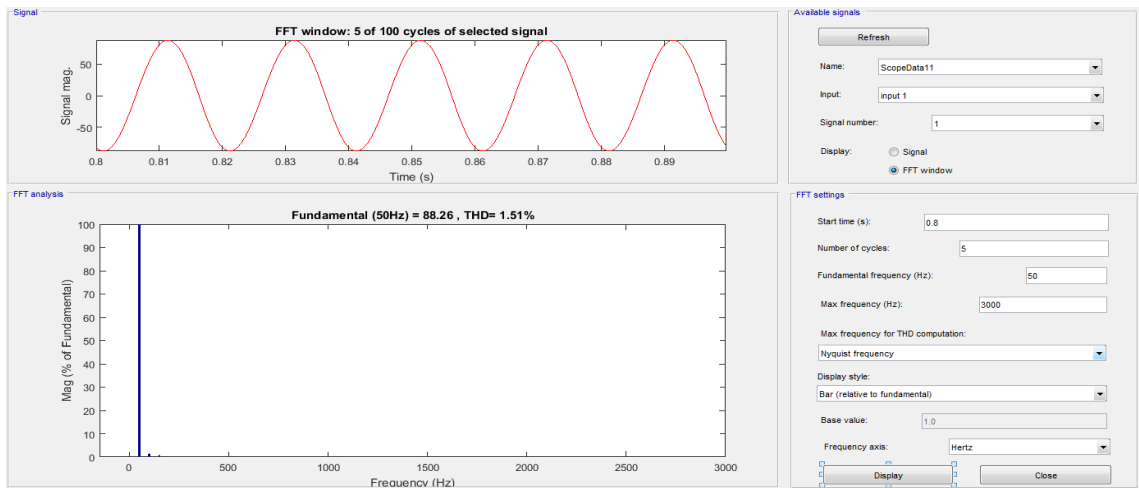
Figure 36 Analysis of R- φ current a) R-phase current waveform b) Harmonic profile of R-φ current

From the above figure it is easily deduced that only the fundamental components appear while the harmonic contents are completely removed.

The contents of Y-φ and B-φ are given in Appendix-VII and VIII.

5. CONCLUSION

This thesis has given a broad review about the concept, theory and basic principle of multilevel inverter. After careful consideration between different modulation techniques, it is concluded that the space-vector-pulse-width modulation (SVPWM) is found to be most popular technique. The brief introduction of carrier based modulation technique is also discussed to get better understanding. While comparing the carrier based pulse width modulation and space-vector-pulse-width modulation, SVPWM carries better DC bus utilization causing a better production of fundamental component by means of amplitude. By implementing this technique the amount of total harmonic distortion (THD) is also get reduced. After careful consideration between the two-level and multilevel inverter, multilevel converter carries better utilization of fundamental component and better profile of THD. However, large number of components will utilize. The name multilevel arise from the fact that how many voltage level the output contains? As far as this thesis is concerned, the pole voltage contains three different voltage levels so it is regarded as three-level SVPWM voltage source inverter. The more the number of levels the better the output is. It closely resembles to sinusoidal output. The three-level inverter is also regarded as neutral point clamp inverter which is commonly used for the purpose of variable frequency drive (VFD) applications. This thesis is also supported with complex mathematical calculation and in order to get better understanding of the theory some waveforms have also been drawn.

To prove this theory, some simulations are also been taken into account in MATLAB/SIMULINK. The overview of each block used in this environment is also presented. The results obtained by utilizing practical values of R-L load. The harmonic contents at each output stage are analyzed by utilizing the FFT analysis tool which is incorporated in SimPowerSys tool box.

5.1 Future Work Proposal

- Implementation of this algorithm in over-modulation region.
- Designing of PI controller for dynamic voltage balancing between the capacitors.
- Investigate 3-Level algorithm as an equivalent 2-Level parallel inverter for reducing mathematical calculation.
- Further implementing THD reduction methods.
- Implementation of Selective Harmonic Elimination (SHE) technique to reduce higher order harmonics.
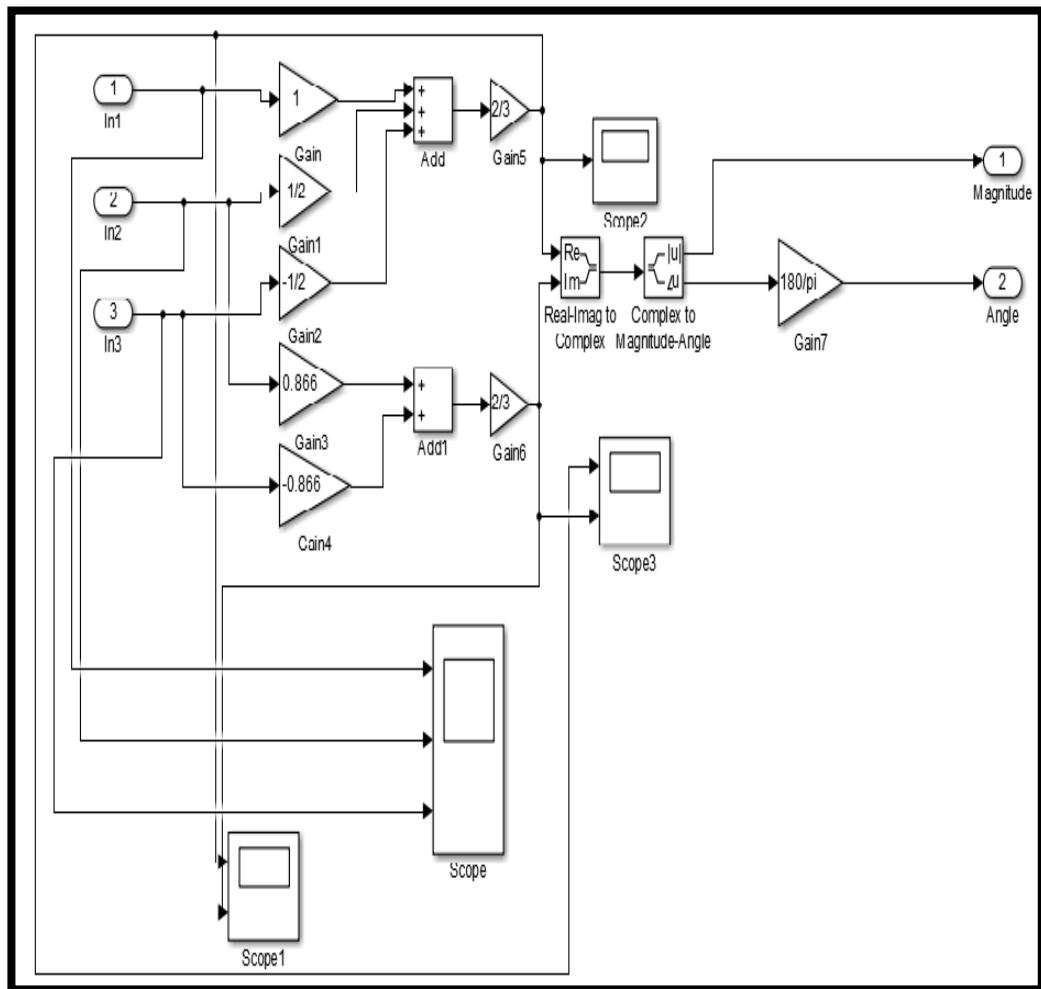
REFERENCES

[1] Mitosz Miskiewicz, Arnstein Johannesen, "A Three-Level Space Vector Modulation Strategy for Two-Level Parallel Inverters", M.S thesis, Inst. of Energy Tech., Aalborg Univ., Denmark, 2009.

[2] Bimal K. Bose, (2002), *Modern Power Electronics and AC Drives*, Prentice Hall, New Jersey

[3] Weixing Feng, "Space Vector Modulation for Three-Level Neutral Point Clamped Inverter", M.Sc Thesis, ECE, Ryerson Univ., Toronto, Canada, 2004.

[4] P. Tripura, Y.S.Kishore Babu, Y.R.Tagore, " Space Vector Pulse Width Modulation Schemes for Two-Level Voltage Source Inverter", Vignan's Nirula Inst. of Tech. & Science, EEE Dept., India, Vignan Univ. Vadlamudi, School of Elect. Eng., India, ACEEE Int. J. on Control System and Instrumentation, Vol. 02, No.3, Oct. 2011.

[5] Dr. Yashvant Jani, Graeme Clark, Renesas Electronics, "MCU with FPU allows advanced Motor Control Solutions", http://www.powersystemsdesign.com/mcu-with-fpu-allows-advanced-motor-control-solutions, 24 April, 2012.

[6] ABD Almula G. M. Gebreel, "Simulation and Implementation of Two Level and Three-Level Inverters by MATLAB and RT-LAB", M.S thesis, ECS, Ohio State Univ., 2011.

[7] *SimPowerSystems For Use with Simulink*, User's Guide, Version 3, Sept. 2003

[8] Suresh L., Mahesh K., Janardhna M. and Mahesh M., "Simulation of Space Vector Pulse Width Modulation for Voltage Source Inverter Using MATLAB/Simulink", J. Automation & Systems Engineering, 133-140, March 2014.

[9] S. Manivannan, S. Veerakumar, P. Karuppusamy, A. Nandhakumar, "Performance Analysis of Three Phase Voltage Source Inverter Fed Induction Motor Drive with Possible Switching Sequence Execution in SVPWM", IJAREEIE, Vol.3, Issue 6, June 2014.

[10] Bimal K. Bose, *Modern Power Electronics and AC Drives*. New Jersey: Prentice Hall, 2002.

[11] Vieri Xue, "Center-Aligned SVPWM Realization for 3- Phase 3- Level Inverter", Application Report, Texas Inst., Oct. 2012

[12] Atif Iqbal, Adoum Lamine, Imtiaz Ashraf, Mohibullah, "MATLAB/SIMULINK MODEL OF SPACE VECTOR PWM FOR THREE-PHASE VOLTAGE

SOURCE INVERTER", Aligarh Muslim Univ. India, Liverpool John Moores Univ. U.K.

[13] D.W. Kang, C.S. Ma, T.J. Kim and D.S. Hyun, "Simple control strategy for balancing the DC-link voltage of neutral-point-clamped inverter at low modulation index", IEE Proc.-Electr. Power Appl., Vol. 151, No. 5, September 2004.

[14] T. Abdelkrim, E.M. Berkouk, Aeh. Benkhelifa, K. Benamrane, T. Benslimane, "Neutral Point Potential Balancing Algorithm for Autonomous Three-Level Shunt Active Power Filter", ARU on Renewable Energies, Ghardaïa, Algeria, Lab. of Process Control, PNS, Algiers, Algeria, LAEIE Uni. of BoumerdesUni of M'sila, Algeria.

[15] K Abhishekam, K Sri Gowri, "Simplified Space Vector PWM Algorithm for a Three Level Inverter", Innovative Systems Design and Eng., ISSN 2222-1727, Vol. 6, No.2, 2015.

[16] Ayse Kocalmis, Sedat Sunter, "Simulation of a Space Vector PWM Controller for a Three –Level Voltage –Fed Inverter Motor Drive," pp.1915-1920.

[17] Mahmoud Kassas, Naseer Ahmed, "Simulation and Implementation of Space Vector PWM Using Look-Up Table", Arab J Sci. Eng.(2014) 39:4815-4828.

[18] Dong-Myung Lee, Jin-Woo Jung, Sang-Shin Kwak, "Simple Space Vector PWM Scheme for 3-Level NPC Inverters Including the Overmodulation Region", Journal of Power Electronics, Vol.11, No.5, Sept. 2011.

[19] Nashiren F. Mailah, Senan M. Bashi, Ishak Aris, Norman Mariun, "Neutral-Point-Clamped Multilevel Inverter Using Space Vector Modulation", European Journal of Scientific research, ISSN 1450-216X, Vol.28 No.1, pp.82-91, 2009.

[20] B.Urmila, D. Subba Rayudu, "Optimum Space Vector PWM Algorithm for Three-Level Inverter", ARPN Journal of Eng. And Applied Sciences, VOL.6, No.9, Sept. 2011.

[21] Sveinung Floten, Tor Stian Haug, "Modulation Methods for Neutral-Point-clamped Three-Level Inverter", M.Sc Thesis, Elec. Power Eng., NTNU, June 2010.

[22] K.Gopala Krishna, T. Kranthi Kumar, and P. Venugopal Rao "Better DC Bus Utilization and Torque Ripple Reduction by using SVPWM for VSI fed Induction Motor Drive", International Journal of Computer and Electrical Engineering, Vol.4, No.2, April 2012.

6. APPENDICES

Appendix I: Implementation of the conversion of three phase quantities to stationary reference frame
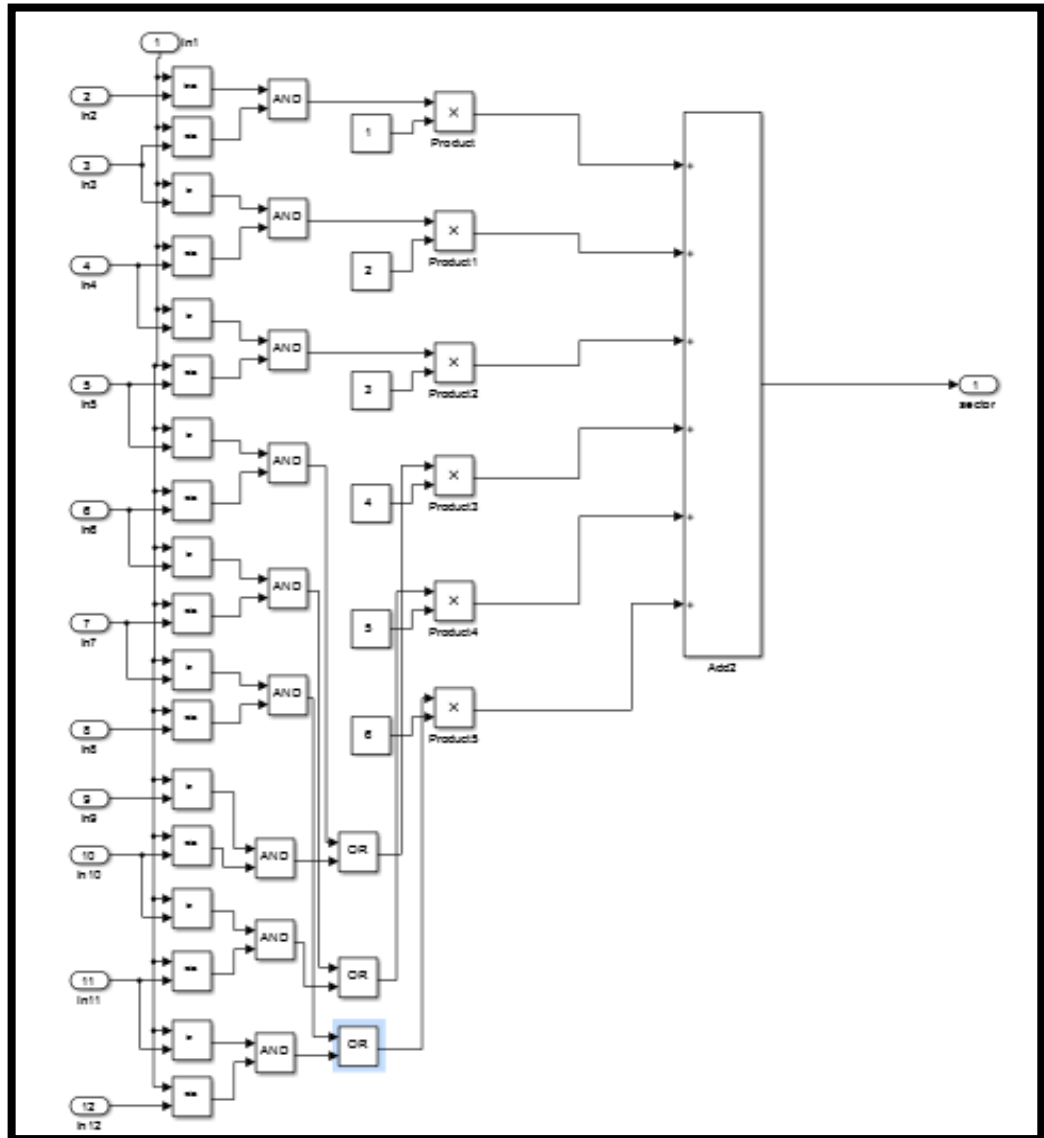
Appendix II: Mathematical model of "Sector Selection" block
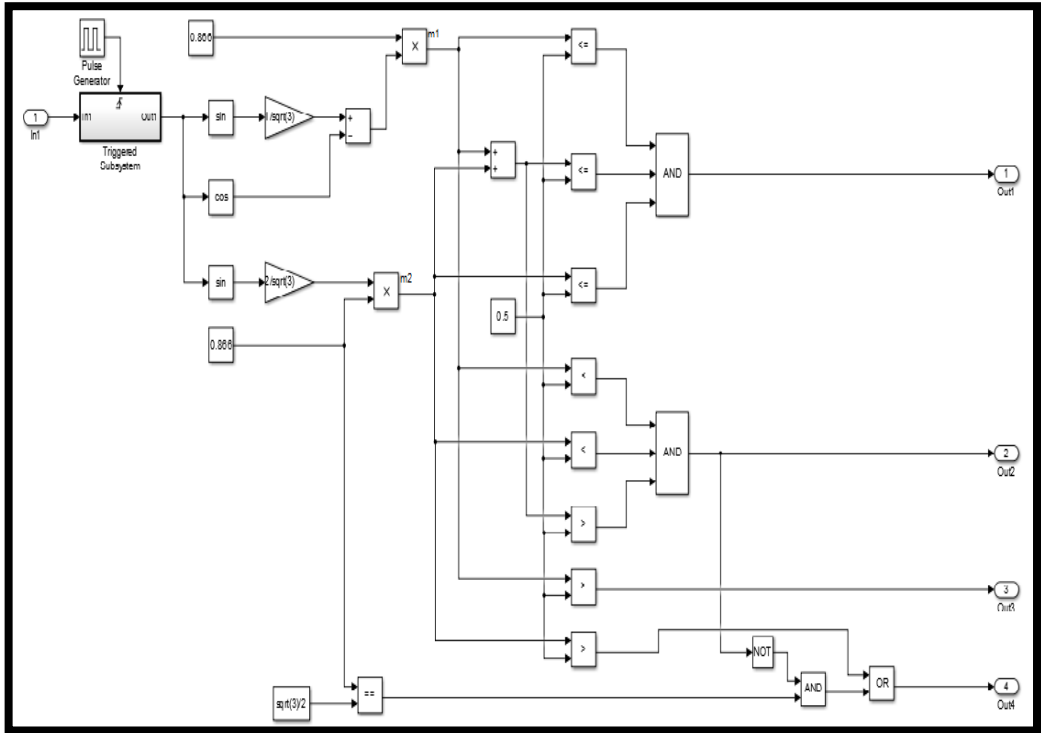
Appendix III: Mathematical model of "Region selection" block
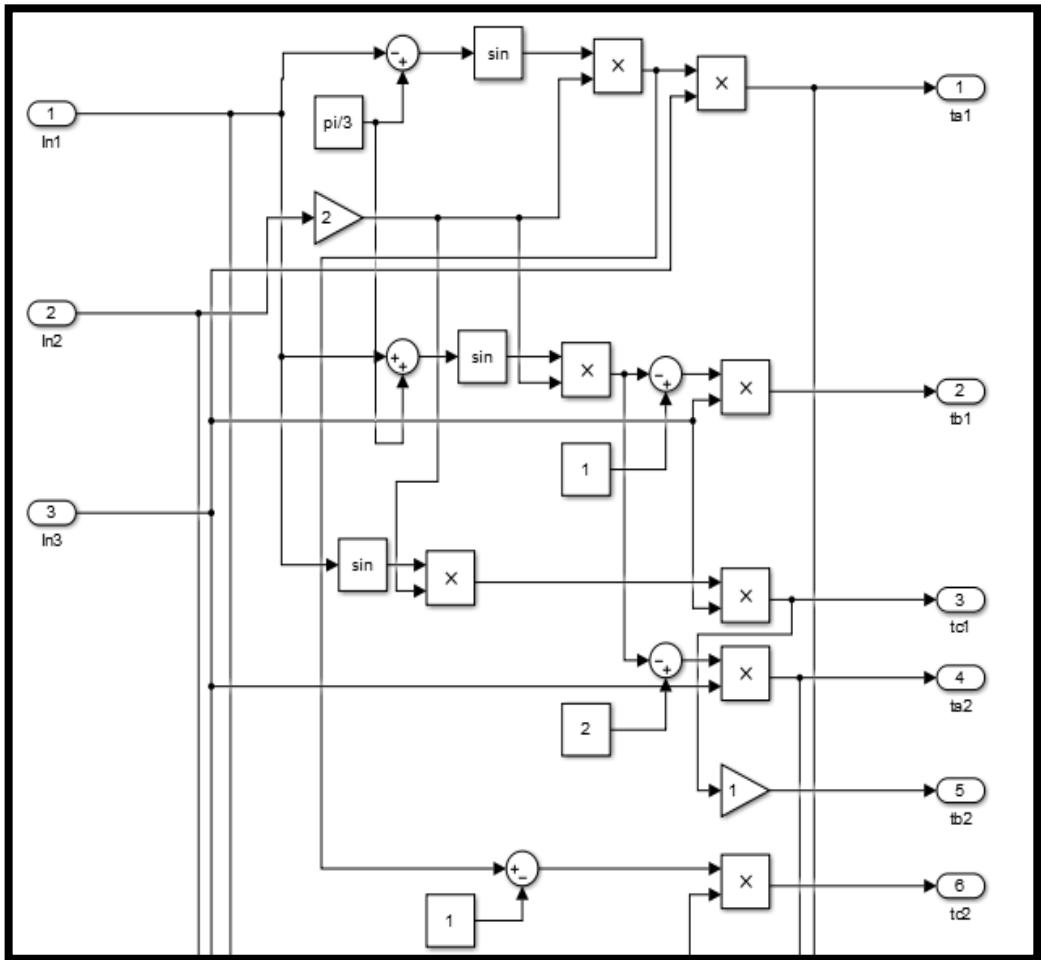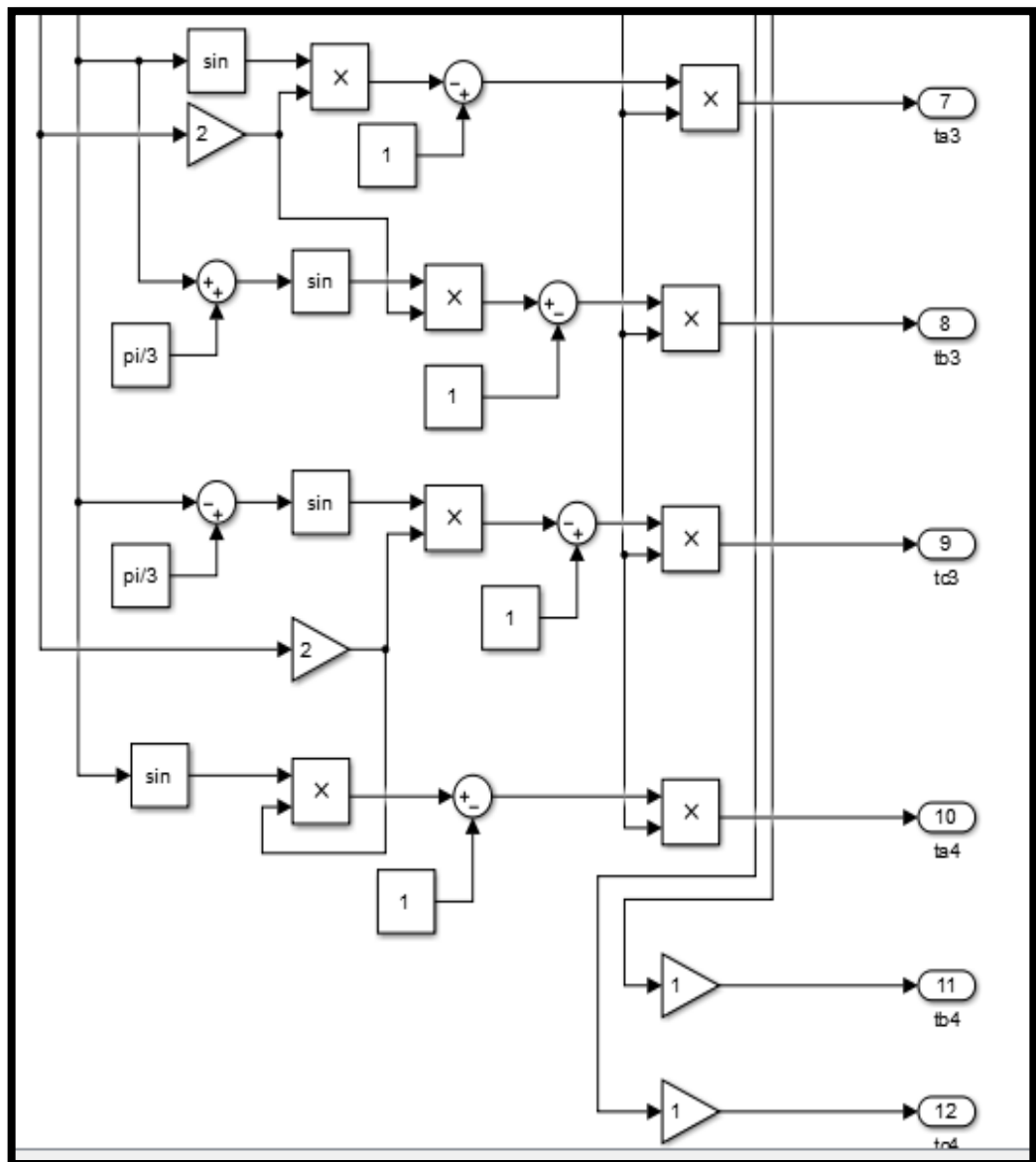
Appendix IV: Mathematical model of "Dwell time calculation" block

a)
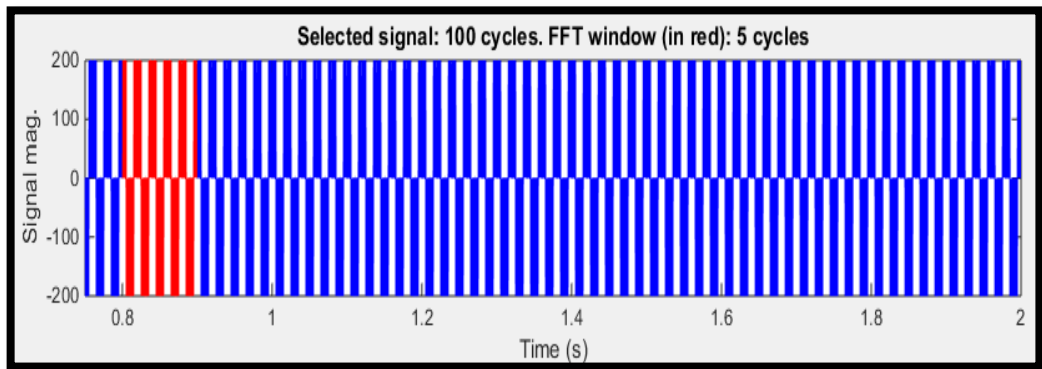
b)
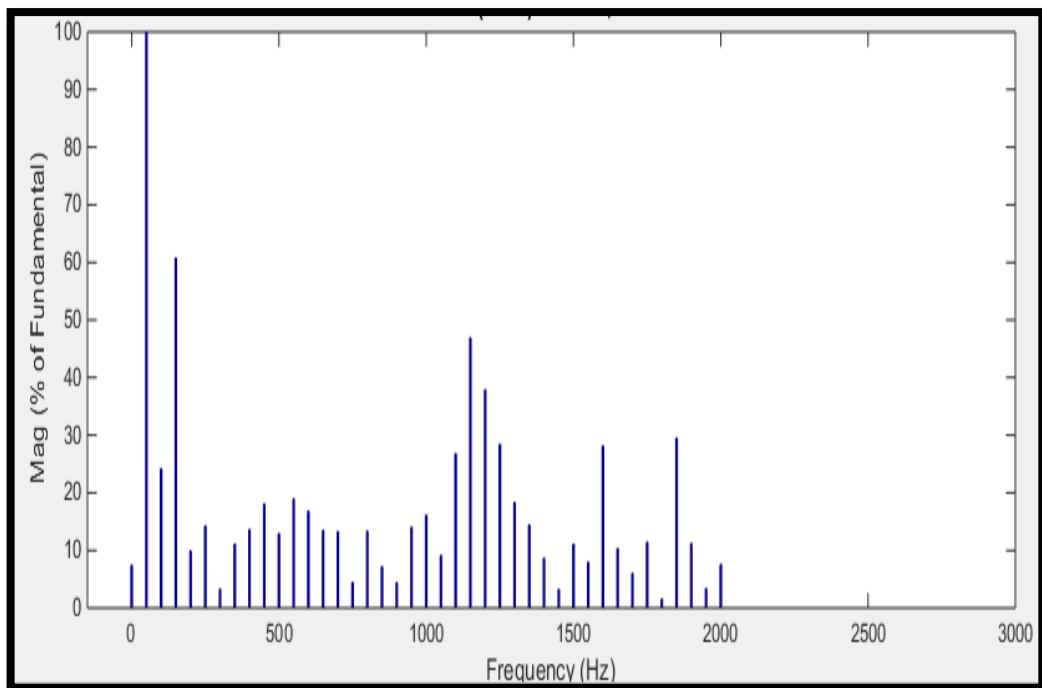
Appendix V: Analysis of Y-φ a) FFT window of Y-phase b) Harmonic analysis of Y-phase

a)
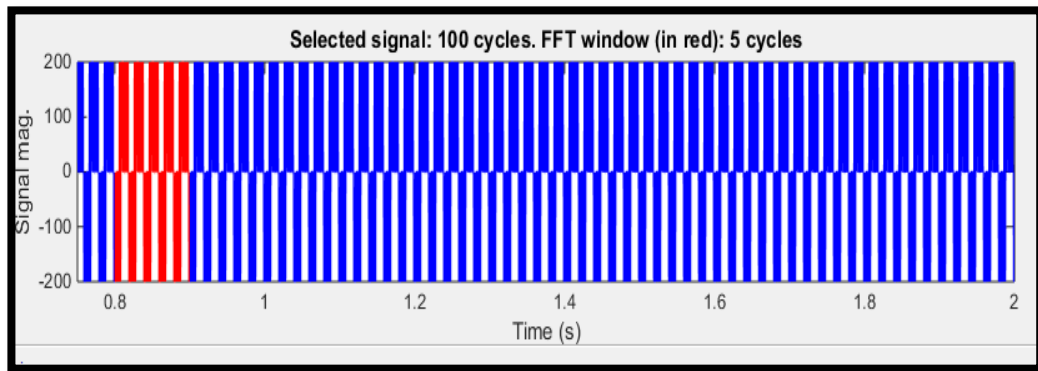
b)
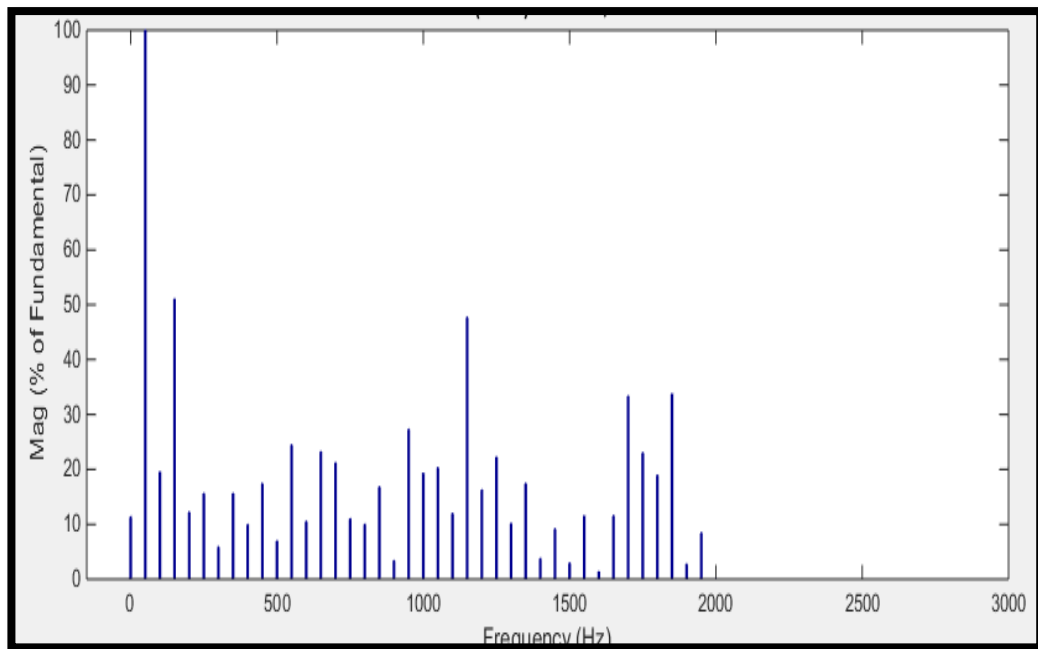
Appendix VI: Analysis of B-φ a) FFT window of B-phase b) Harmonic analysis of B-phase

a)
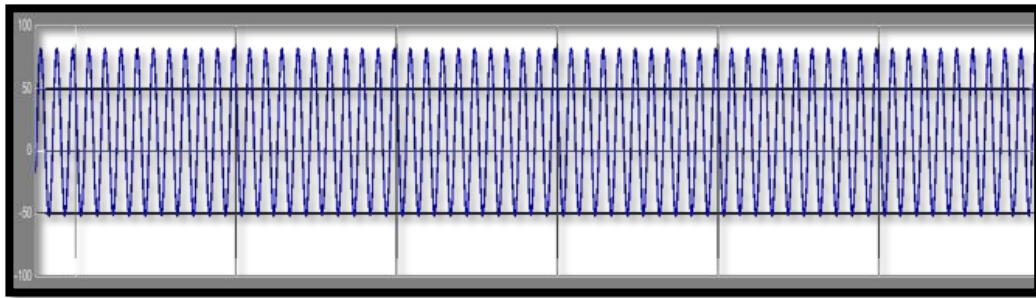
b)
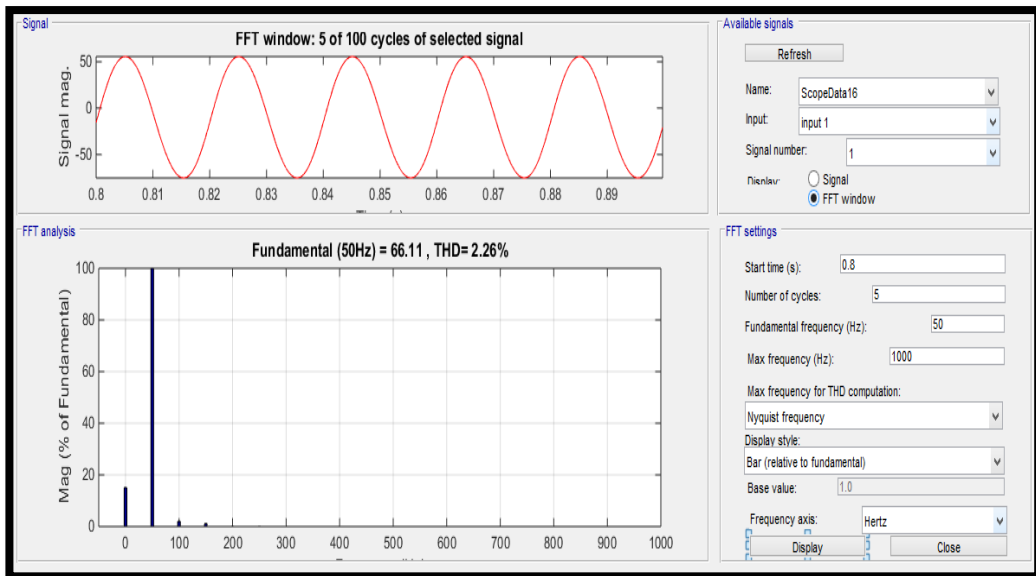
***Appendix VII: Analysis of Y-Phase current a) current waveform b) Harmonic
analysis***

a)

b)

Appendix VIII: Analysis of B-Phase current a) current waveform b) Harmonic analysis

13-Segment Scheme

S2,R1	V_{27}	V_7	V_{12}	V_1	V_8	V_{13}	V_2	V_{13}	V_8	V_1	V_{12}	V_7	V_{27}
	+++	+++	0+0	000	00-	-0-	---	-0-	00-	000	0+0	++0	+++
	$\frac{T_b}{8}$	$\frac{T_c}{4}$	$\frac{T_b}{4}$	$\frac{T_b}{4}$	$\frac{T_c}{4}$	$\frac{T_a}{4}$	$\frac{T_b}{4}$	$\frac{T_a}{4}$	$\frac{T_c}{4}$	$\frac{T_b}{4}$	$\frac{T_a}{4}$	$\frac{T_c}{4}$	$\frac{T_b}{8}$

S3,R1	V_2	V_{13}	V_{15}	V_1	V_{12}	V_{14}	V_{27}	V_{14}	V_{12}	V_1	V_{15}	V_{13}	V_2
	---	-0-	-00	000	0+0	0++	+++	0++	0+0	000	-00	-0-	---
	$\frac{T_b}{8}$	$\frac{T_a}{4}$	$\frac{T_c}{4}$	$\frac{T_b}{4}$	$\frac{T_a}{4}$	$\frac{T_c}{4}$	$\frac{T_b}{4}$	$\frac{T_c}{4}$	$\frac{T_a}{4}$	$\frac{T_b}{4}$	$\frac{T_c}{4}$	$\frac{T_a}{4}$	$\frac{T_b}{8}$

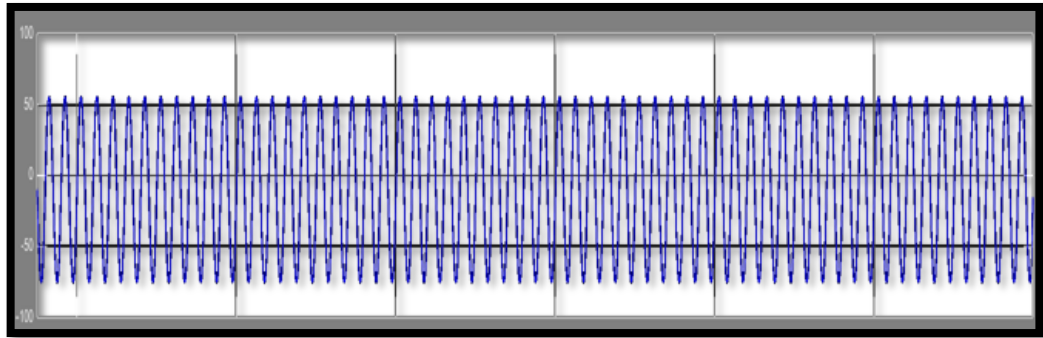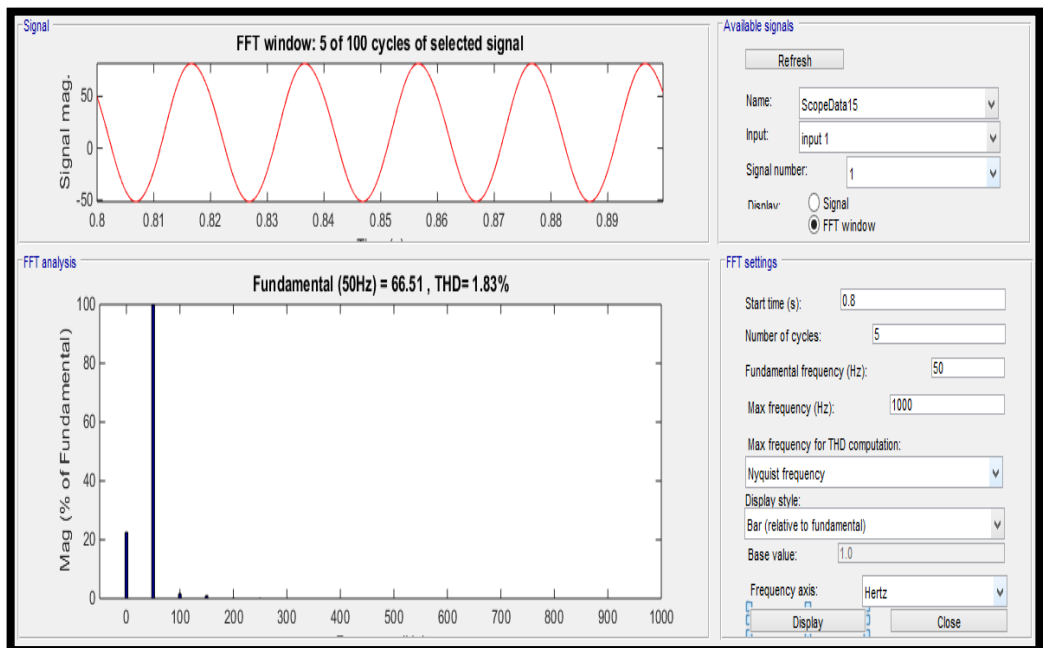| S4,R1	V_{27}	V_{14}	V_{19}	V_1	V_{15}	V_{20}	V_2	V_{20}	V_{15}	V_1	V_{19}	V_{14}	V_{27}
	+++	0++	00+	000	-00	--0	---	--0	-00	000	00+	0++	+++
	$\frac{T_b}{8}$	$\frac{T_c}{4}$	$\frac{T_a}{4}$	$\frac{T_b}{4}$	$\frac{T_c}{4}$	$\frac{T_a}{4}$	$\frac{T_b}{4}$	$\frac{T_a}{4}$	$\frac{T_c}{4}$	$\frac{T_b}{4}$	$\frac{T_a}{4}$	$\frac{T_c}{4}$	$\frac{T_b}{8}$

S5,R1	V_2	V_{20}	V_{24}	V_1	V_{19}	V_{23}	V_{27}	V_{23}	V_{19}	V_1	V_{24}	V_{20}	V_2
	---	--0	0-0	000	00+	+0+	+++	+0+	00+	000	0-0	--0	---
	$\frac{T_b}{8}$	$\frac{T_a}{4}$	$\frac{T_c}{4}$	$\frac{T_b}{4}$	$\frac{T_a}{4}$	$\frac{T_c}{4}$	$\frac{T_b}{4}$	$\frac{T_c}{4}$	$\frac{T_a}{4}$	$\frac{T_b}{4}$	$\frac{T_c}{4}$	$\frac{T_a}{4}$	$\frac{T_b}{8}$

S6,R1	V_{27}	V_{23}	V_3	V_1	V_{24}	V_4	V_2	V_4	V_{24}	V_1	V_3	V_{23}	V_{27}
	+++	+0+	+00	000	0-0	0--	---	0--	0-0	000	+00	+0+	+++
	$\frac{T_b}{8}$	$\frac{T_c}{4}$	$\frac{T_a}{4}$	$\frac{T_b}{4}$	$\frac{T_c}{4}$	$\frac{T_a}{4}$	$\frac{T_b}{4}$	$\frac{T_a}{4}$	$\frac{T_c}{4}$	$\frac{T_b}{4}$	$\frac{T_a}{4}$	$\frac{T_c}{4}$	$\frac{T_b}{8}$

7-Segment Scheme							
S2,R2	V_7	V_9	V_{10}	V_8	V_{10}	V_9	V_7
	++0	++-	0+-	00-	0+-	++-	++0
	$\dfrac{T_c}{4}$	$\dfrac{T_a}{2}$	$\dfrac{T_b}{2}$	$\dfrac{T_c}{2}$	$\dfrac{T_b}{2}$	$\dfrac{T_a}{2}$	$\dfrac{T_c}{4}$
S3,R2	V_{13}	V_{11}	V_{16}	V_{12}	V_{16}	V_{11}	V_{13}
	-0-	-+-	-+0	0+0	-+0	-+-	-0-
	$\dfrac{T_a}{4}$	$\dfrac{T_c}{2}$	$\dfrac{T_b}{2}$	$\dfrac{T_a}{2}$	$\dfrac{T_b}{2}$	$\dfrac{T_c}{2}$	$\dfrac{T_a}{4}$
S4,R2	V_{14}	V_{17}	V_{18}	V_{15}	V_{18}	V_{17}	V_{14}
	0++	-++	-0+	-00	-0+	-++	0++
	$\dfrac{T_c}{4}$	$\dfrac{T_a}{2}$	$\dfrac{T_b}{2}$	$\dfrac{T_c}{2}$	$\dfrac{T_b}{2}$	$\dfrac{T_a}{2}$	$\dfrac{T_c}{4}$
S5,R2	V_{20}	V_{21}	V_{22}	V_{19}	V_{22}	V_{21}	V_{20}
	--0	--+	0-+	00+	0-+	--+	--0
	$\dfrac{T_a}{4}$	$\dfrac{T_c}{2}$	$\dfrac{T_b}{2}$	$\dfrac{T_a}{2}$	$\dfrac{T_b}{2}$	$\dfrac{T_c}{2}$	$\dfrac{T_a}{4}$
S6,R2	V_{23}	V_{25}	V_{26}	V_{24}	V_{26}	V_{25}	V_{23}
	+0+	+-+	+-0	0-0	+-0	+-+	+0+
	$\dfrac{T_c}{4}$	$\dfrac{T_a}{2}$	$\dfrac{T_b}{2}$	$\dfrac{T_c}{2}$	$\dfrac{T_b}{2}$	$\dfrac{T_a}{2}$	$\dfrac{T_c}{4}$

9-Segment Scheme

|									
S2,R3	V_7	V_{12}	V_{10}	V_8	V_{13}	V_8	V_{10}	V_{12}	V_7
	++0	0+0	0+-	00-	-0-	00-	0+-	0+0	++0
	$\frac{T_c}{4}$	$\frac{T_a}{4}$	$\frac{T_b}{2}$	$\frac{T_c}{4}$	$\frac{T_a}{2}$	$\frac{T_c}{4}$	$\frac{T_b}{2}$	$\frac{T_a}{4}$	$\frac{T_c}{4}$
S3,R3	V_{13}	V_{15}	V_{16}	V_{12}	V_{14}	V_{12}	V_{16}	V_{15}	V_{13}
	-0-	-00	-+0	0+0	0++	0+0	-+0	-00	-0-
	$\frac{T_a}{4}$	$\frac{T_c}{4}$	$\frac{T_b}{2}$	$\frac{T_a}{4}$	$\frac{T_c}{2}$	$\frac{T_a}{4}$	$\frac{T_b}{2}$	$\frac{T_c}{4}$	$\frac{T_a}{4}$
S4,R3	V_{14}	V_{19}	V_{18}	V_{15}	V_{20}	V_{15}	V_{18}	V_{19}	V_{14}
	0++	00+	-0+	-00	--0	-00	-0+	00+	0++
	$\frac{T_c}{4}$	$\frac{T_a}{4}$	$\frac{T_b}{2}$	$\frac{T_c}{4}$	$\frac{T_a}{2}$	$\frac{T_c}{4}$	$\frac{T_b}{2}$	$\frac{T_a}{4}$	$\frac{T_c}{4}$
S5,R3	V_{20}	V_{24}	V_{22}	V_{19}	V_{23}	V_{19}	V_{22}	V_{24}	V_{20}
	--0	0-0	0-+	00+	+0+	00+	0-+	0-0	--0
	$\frac{T_a}{4}$	$\frac{T_c}{4}$	$\frac{T_b}{2}$	$\frac{T_a}{4}$	$\frac{T_c}{2}$	$\frac{T_a}{4}$	$\frac{T_b}{2}$	$\frac{T_c}{4}$	$\frac{T_a}{4}$
S6,R3	V_{23}	V_3	V_{26}	V_{24}	V_4	V_{24}	V_{26}	V_3	V_{23}
	+0+	++0	+-0	0-0	0--	0-0	+-0	+00	+0+
	$\frac{T_c}{4}$	$\frac{T_a}{4}$	$\frac{T_b}{2}$	$\frac{T_c}{4}$	$\frac{T_a}{2}$	$\frac{T_c}{4}$	$\frac{T_b}{2}$	$\frac{T_a}{4}$	$\frac{T_c}{4}$

				7-Segment Scheme			
S2,R4	V_{12}	V_{10}	V_{11}	V_{13}	V_{11}	V_{10}	V_{12}
	0+0	0+-	-+-	-0-	-+-	0+-	0+0
	$\dfrac{T_a}{4}$	$\dfrac{T_b}{2}$	$\dfrac{T_c}{2}$	$\dfrac{T_a}{2}$	$\dfrac{T_c}{2}$	$\dfrac{T_b}{2}$	$\dfrac{T_a}{4}$
S3,R4	V_{15}	V_{16}	V_{17}	V_{14}	V_{17}	V_{16}	V_{15}
	-00	-+0	-++	0++	-++	-+0	-00
	$\dfrac{T_c}{4}$	$\dfrac{T_b}{2}$	$\dfrac{T_a}{2}$	$\dfrac{T_c}{2}$	$\dfrac{T_a}{2}$	$\dfrac{T_b}{2}$	$\dfrac{T_c}{4}$
S4,R4	V_{19}	V_{18}	V_{21}	V_{20}	V_{21}	V_{18}	V_{19}
	00+	-0+	--+	--0	--+	-0+	00+
	$\dfrac{T_a}{4}$	$\dfrac{T_b}{2}$	$\dfrac{T_c}{2}$	$\dfrac{T_a}{2}$	$\dfrac{T_c}{2}$	$\dfrac{T_b}{2}$	$\dfrac{T_a}{4}$
S5,R4	V_{24}	V_{22}	V_{25}	V_{23}	V_{25}	V_{22}	V_{24}
	0-0	0-+	+-+	+0+	+-+	0-+	0-0
	$\dfrac{T_c}{4}$	$\dfrac{T_b}{2}$	$\dfrac{T_a}{2}$	$\dfrac{T_c}{2}$	$\dfrac{T_a}{2}$	$\dfrac{T_b}{2}$	$\dfrac{T_c}{4}$
S6,R4	V_3	V_{26}	V_5	V_4	V_5	V_{26}	V_3
	+00	+-0	+--	0--	+--	+-0	+00
	$\dfrac{T_a}{4}$	$\dfrac{T_b}{2}$	$\dfrac{T_c}{2}$	$\dfrac{T_a}{2}$	$\dfrac{T_c}{2}$	$\dfrac{T_b}{2}$	$\dfrac{T_a}{4}$

Appendix IX: Switching schemes for sector II, III, IV, V and VI

a)
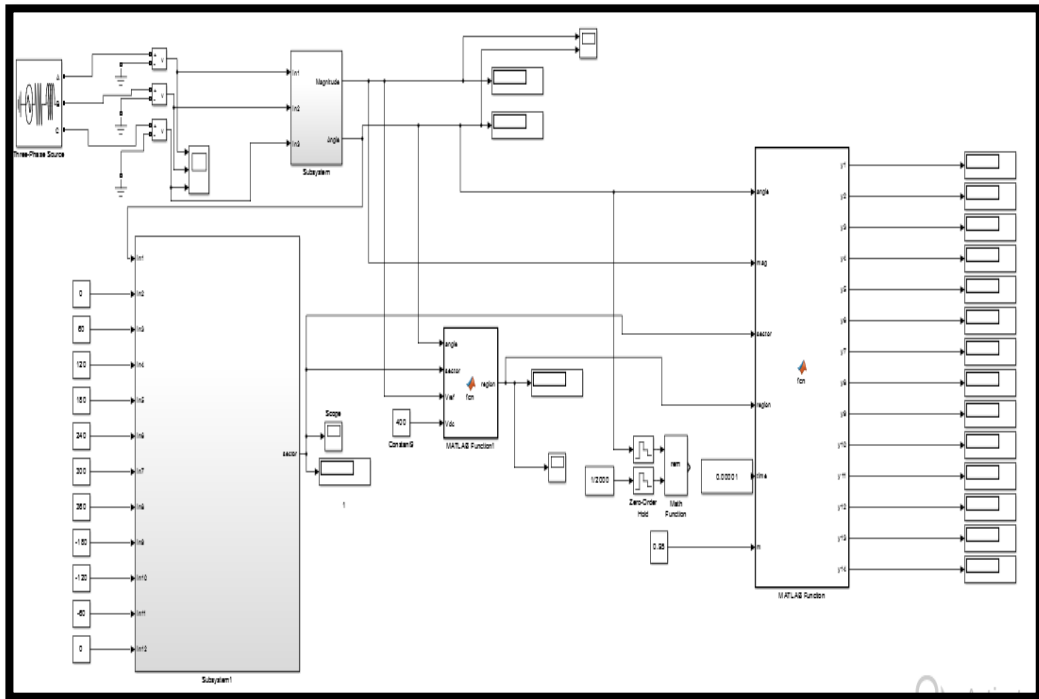
b)
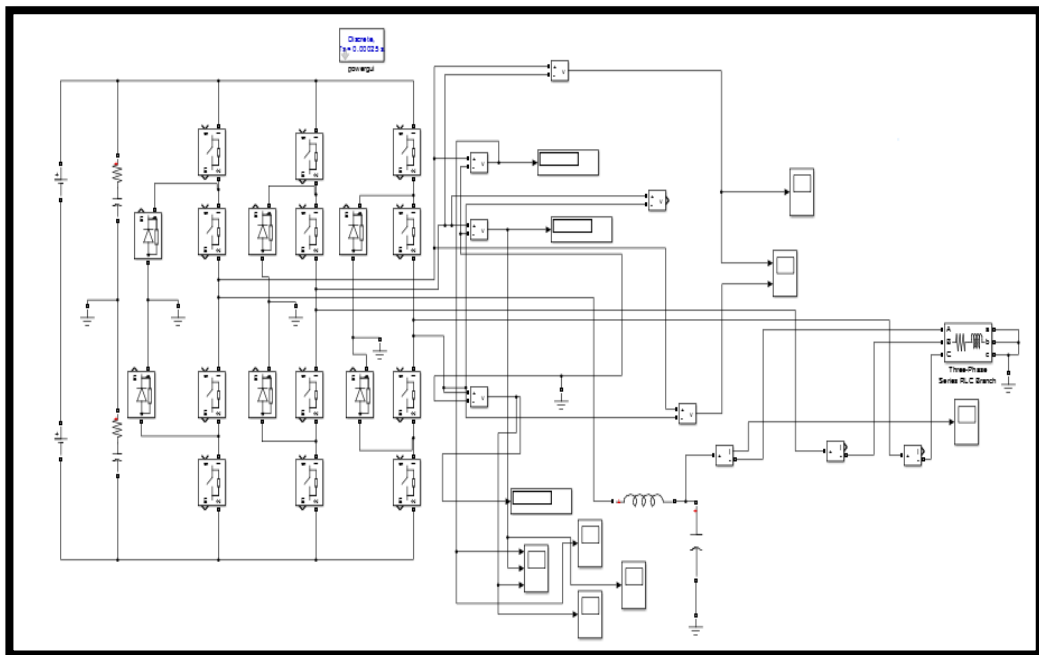
Appendix IX: a) Simulink model of 3-level inverter b) power stage of the inverter